

# **VIIRS Snow Cover Algorithm Theoretical Basis Document (ATBD)**

Science Principal Investigator: Dr. Dorothy K Hall

Correspondence e-mail address: [Dorothy.K.Hall@nasa.gov](mailto:Dorothy.K.Hall@nasa.gov)

Prepared by George Riggs, Dorothy Hall, and Miguel O. Román

Version 1.0

December 18<sup>th</sup> 2015

**NASA Goddard Space Flight Center**

**Greenbelt, Maryland**

# Table of Contents

<b>1.0 Introduction .....</b>	<b>3</b>
<b>1.1 Science/Applications Rationale for the Product.....</b>	<b>3</b>
<b>1.2 Intended user community.....</b>	<b>3</b>
<b>2.0 Algorithm Description .....</b>	<b>5</b>
<b>2.1 Technical Background and Heritage .....</b>	<b>5</b>
2.1.1 Snow Cover Extent based on NDSI.....	7
<b>2.2 Algorithm Description (The Normalized Difference Snow Index (NDSI)).....</b>	<b>8</b>
2.2.1 Algorithm Limitations.....	17
2.2.2 Algorithm Flow .....	18
<b>2.3 Product Description.....</b>	<b>18</b>
<b>3.0 Product Inputs .....</b>	<b>20</b>
<b>3.1 Spectral Bands.....</b>	<b>21</b>
<b>3.2 Masks, Thresholds and Ancillary Data .....</b>	<b>21</b>
<b>4.0 Product Accuracy/Uncertainty .....</b>	<b>29</b>
<b>4.1 Uncertainty Estimate.....</b>	<b>31</b>
<b>4.2 Validation Approach.....</b>	<b>32</b>
<b>5.0 Data Format .....</b>	<b>33</b>
<b>5.1 Format .....</b>	<b>33</b>
<b>5.2 QA Metadata .....</b>	<b>33</b>
<b>6.0 Product Publications .....</b>	<b>34</b>
<b>7.0 References.....</b>	<b>34</b>

## **1.0 INTRODUCTION**

The importance of monitoring snow cover onset, duration and melt at local, regional and global scales and for climate and hydrologic applications at local and regional scales has been documented in many studies. The Suomi-NPP (S-NPP) Visible Infrared Imaging Radiometer Suite (VIIRS) snow cover algorithm and data products have been developed for analysis of snow cover at local to global scales. Daily monitoring of snow cover requires a robust algorithm that can provide accurate results in all conditions spatially and temporally from ideal to the most challenging viewing situations. The heritage Moderate Resolution Imaging Spectroradiometer (MODIS) snow cover algorithm and data products have been used extensively at local, regional and global scales by numerous researches in many different countries and are used as the foundation of the VIIRS snow cover algorithm and product. The theory of the normalized difference snow index (NDSI) technique for snow detection is discussed followed by description of the algorithm and data product then the accuracy and uncertainty of the algorithm and product and validation approach are presented. Information on the data product format is also given.

### **1.1 Science/Applications Rationale for the Product**

Many studies using satellite and in-situ data show that Northern Hemisphere snow cover extent and timing of snow melt are changing (Choi et al., 2010, Brown and Robinson, 2011; Robinson and Estilow, 2013). Derksen and Brown (2012) and Brown et al. (2010) found that snow cover melt is occurring earlier in the spring at some locations in the Northern Hemisphere. Spring snow cover has undergone significant reductions over the past 90 years and the rate of decrease has accelerated over the past 40 years. Results from the Rutgers Global Snow Lab snow cover climate-data record (CDR) <http://climate.rutgers.edu/snowcover> for the nearly 50- record, show an earlier spring snowmelt in the Northern Hemisphere of  $-2.12 \pm 0.45\%$ /decade. MODIS snow-cover products have been used to study trends or interannual variability in snow cover (e.g., Pu et al., 2007), and for developing snow-cover depletion curves for hydrologic modeling and for other investigations and applications. A listing of citations is maintained on our project website <http://modis-snow-ice.gsfc.nasa.gov/?c=publications> which contains more than 260 citations for the standard MODIS snow products.

### **1.2 Intended user community**

The S-NPP snow cover algorithm and data products will extend the Earth Observing System (EOS) snow cover data product record. The NASA EOS MODIS snow cover data record that began in 2000 has been used in a range of research and applications to monitor snow cover onset, duration, and melt date in studies ranging from synoptic study of snow cover related to climate change to monitoring of watershed snow cover for hydrological modeling. The S-NPP VIIRS snow cover data products may be used to study the occurrence and extent of snow cover across all landscapes in ways similar to those of MODIS.

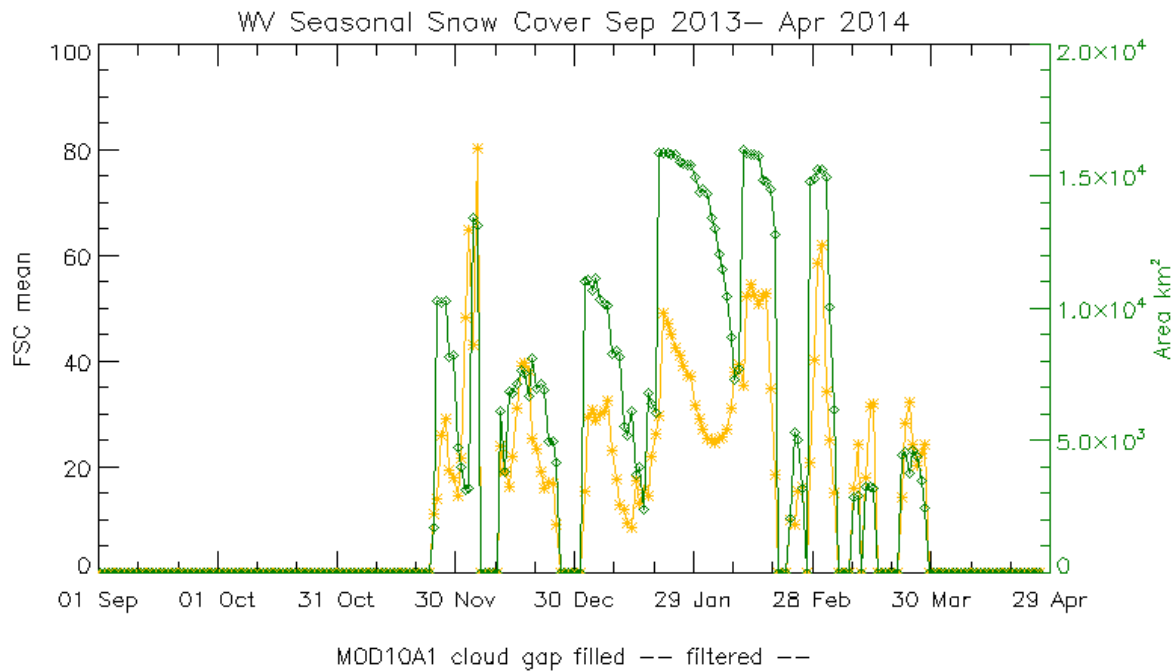


Figure 1. Seasonal track of snow cover extent by FSC mean (green) and area (gold) for a region of Appalachian Mountains in WV. The onset of snow cover, duration and melt are accurately observed as are intermittent snow free periods within the snow season (Riggs and Hall, 2014).

MODIS Collection 5 (C5) heritage snow cover data products have been used by Dietz, et al. (2012) to create snow cover duration maps of Europe 2000-2011 using the MODIS Terra (MOD10A1) and Aqua (MYD10A1) data products with assessed accuracy of above 90%. Dietz, et al. (2013) created a snow cover duration map of central Asia for the same period, and detected a north-south gradient in snow cover duration, start and melt. The MODIS snow cover products have also been used to make snow depletion curves in hydrologic studies and modeling on regional scales (e.g., Dèry and Brown, 2007; Hall et al., 2012; Crawford, 2013; Parajka and Blöschl, 2012). The daily MODIS snow cover extent product can be used to accurately track seasonal snow cover on the landscape, as demonstrate for a region of the Appalachian Mountains in West Virginia Fig. 1 (Riggs and Hall, 2014). The snow cover algorithm has been robust across most landscapes and conditions with accuracy estimates of > 80% for most situations and the products have been applied in a variety of research and applications. Similar accuracy and usage is expected for the VIIRS snow cover product. A listing of published papers that have used the MODIS snow products is maintained at the MODIS snow and ice project website, <http://modis-snow-ice.gsfc.nasa.gov/>. The NASA VIIRS snow cover product will continue the EOS snow cover data record that was begun with the Terra MODIS in February 2000 and is expected to have similar robustness and accuracy.

## 2.0 SNOW COVER ALGORITHM

The NASA VIIRS snow cover algorithm uses the normalized difference snow index (NDSI) technique which is effective at detecting snow cover globally with high accuracy over a wide range of viewing conditions. Theory of the NDSI is discussed then limitations, sources of error and implementation of the snow detection algorithm are presented in the following sections.

### 2.1 Technical Background and Heritage

Snow cover reflectance characteristics of high visible (VIS) reflectance across the 0.3 – 1.0  $\mu\text{m}$  wavelengths and low reflectance of shortwave near-infrared (SWIR) reflectance  $\sim 1.6 \mu\text{m}$  are the primary characteristics used to detect snow cover on the landscape using satellite sensors with spectral bands in the visible and infrared wavelength regions. Frei et al. (2012) discuss the reasons for monitoring snow cover with visible, SWIR, and passive microwave sensors, as well as the techniques and algorithms used to generate global scale daily snow cover products. Across the globe, there is a vast range of satellite and solar viewing geometry, illumination, temporal (diurnal and seasonal), and atmospheric conditions (aerosol and cloud) that affect reflectance from snow. The objective is to develop an algorithm that is able to detect snow cover from very low solar viewing angles at the edge of darkness to local solar noon viewing conditions across all landscape conditions that may occur throughout the year.

The snow characteristic of high VIS reflectance and very low SWIR reflectance is seen in the numerous snow reflectance curves reported in the literature using *in situ* measurements acquired with spectrometers in field or laboratory, from airborne or spaceborne hyperspectral sensors or from spectral reflectance modeling. High VIS reflectance and low SWIR reflectance is an intrinsic optical characteristic of snow however, the relative magnitude of VIS and SWIR reflectance difference can vary with snow conditions or illumination. An example of snow reflectance curves for snow of different ages and dirty snow from Punia and Dhankar (2014) is shown in Fig. 2. Snow reflectance curves obtained in the field from spectrometers e.g. Satterwhite et al., (2003), Negi et al. (2010), Zhang et al. (2011) or spaceborne sensors e.g. Punia and Dhankar (2014) all demonstrate this intrinsic property of snow under many different physical snow or illumination/viewing conditions. The theory of using the NDSI for detection of snow cover is based on the difference between high VIS snow reflectance and low SWIR reflectance, ideally under sunlit conditions of pure snow and high solar elevation angle and clear atmosphere when the reflectance difference is large. However snow in other situations, such as low illumination or under vegetation canopy, may exhibit a relatively low reflectance difference, as shown in reports in the literature, which implies that there may be a lower limit to the accuracy or effectiveness of using the NDSI technique.

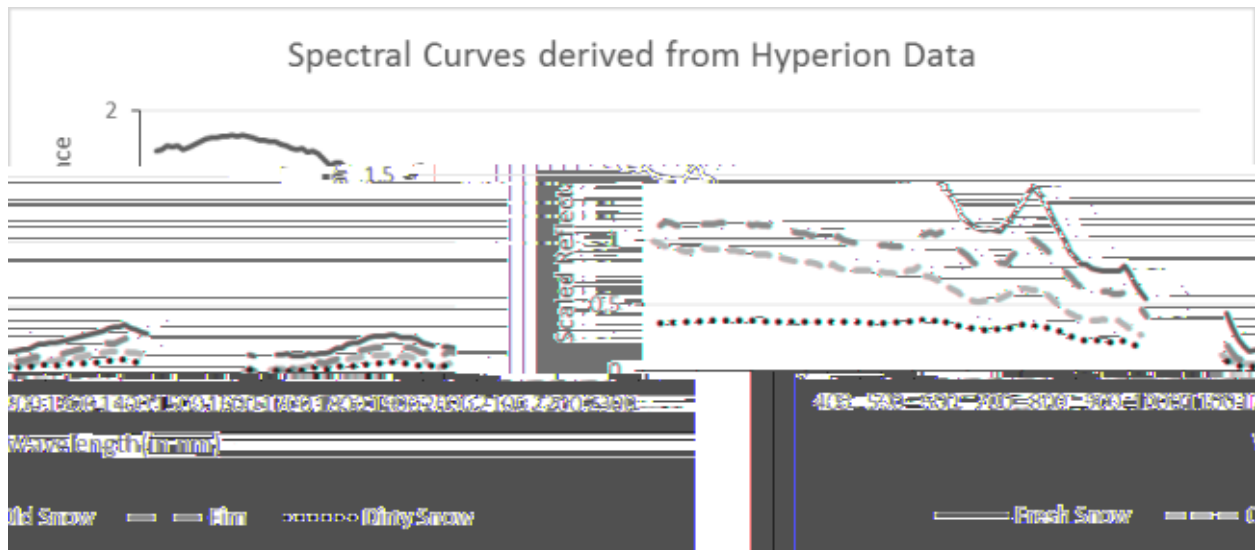


Figure 2. Hyperion acquired snow reflectance curves from Punia and Dhankar (2014) of Himalayan snow cover.

The use of VIS and SWIR reflectance as a ratio or as a normalized difference to detect snow cover has been done since the mid 1970s in various forms with different satellite sensors to reliably and accurately map snow cover. A concise history of the use of VIS to SWIR ratios and the normalized difference snow index (NDSI) is given in Hall and Riggs (2011). The NDSI has been used in the MODIS snow cover product algorithm in all collections since 2000 and is used in the S-NPP VIIRS snow cover product algorithm.

The first intended use of ratios of VIS and NIR or SWIR was to separate snow and clouds in the mid-1970s by Valovcin (1976, 1978) and Kyle et al. (1978) with considerable more work by Bunting and d'Entemont (1982) who developed an automated algorithm to discriminate snow cover from cloud for global cloud analysis. In the 1980s research focused on using the VIR and NIR ratio technique to refine algorithms for snow cover detection with notable contributions by Crane and Anderson (1984), Dozier (1989) with the refinement of using a normalized difference of VIS and NIR, and Rosenthal and Dozier (1996) at regional scales and by Riggs et al (1993), Hall et al (1995, 2002) and Hall and Riggs (2007) for global snow cover mapping. In those techniques, snow covered area (SCA) was determined by setting a threshold value of the ratio or normalized difference to make a binary map of SCA. Determining the NDSI threshold to set for snow detection is a significant decision of many research studies for example Sibandze et al. (2014). Generating SCA maps from the NDSI does not use the full range of information that could be extracted from the NDSI to detect snow cover.

The processing architecture for the NDSI snow cover detection technique is shown in Figure 3. Data required for the algorithm are extracted from the VIIRS inputs and processed then the NDSI is calculated for all daylight pixels in a swath, then data screens are applied and QC flags set. The cloud mask, ocean mask, and night mask are applied to make the NDSI snow cover data set.

layer for output. An unmasked NDSI data layer is also output and the QC data layers are output to the product.

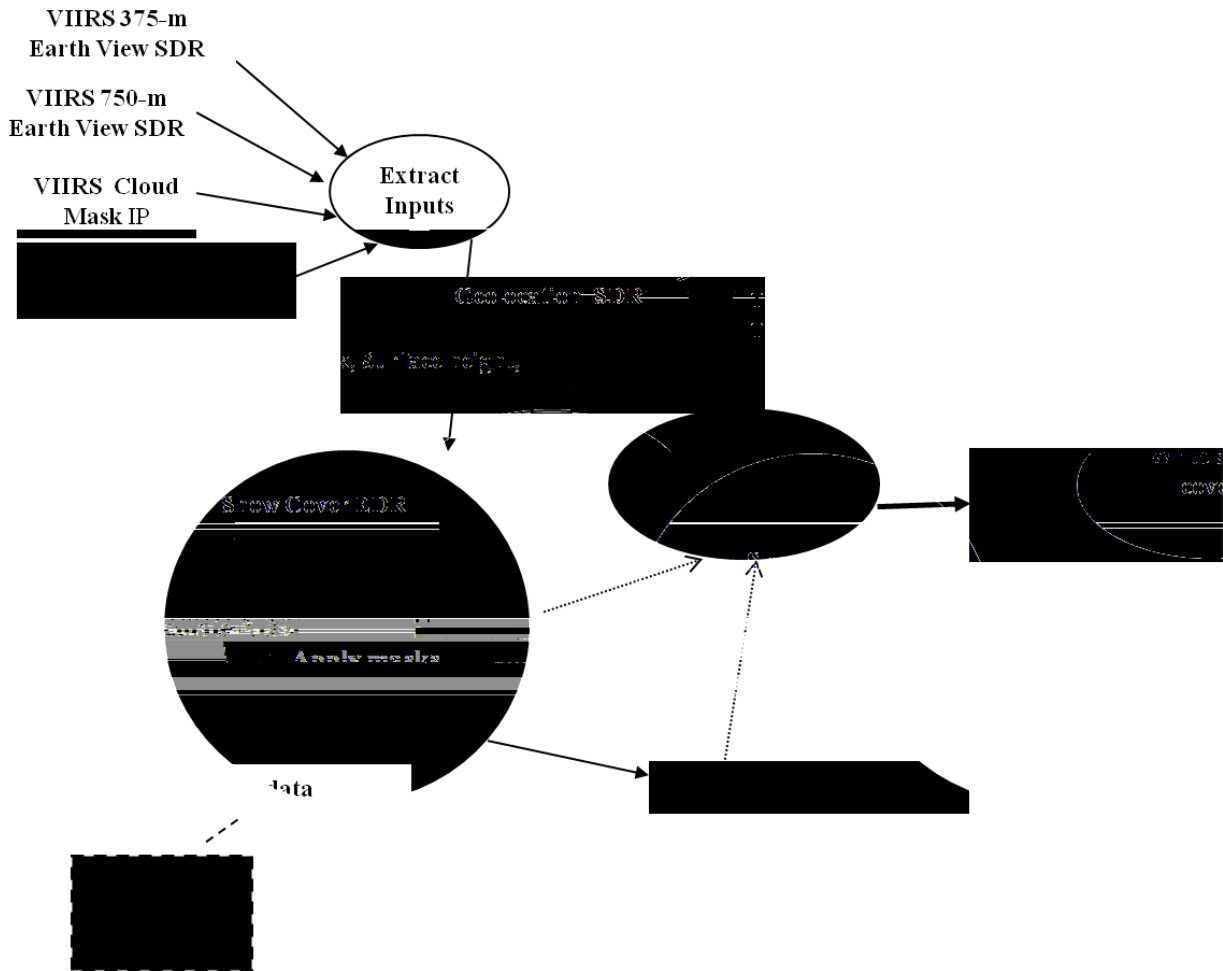


**Figure 3. Snow Cover EDR processing architecture.**

### 2.1.1 Snow Cover Extent based on NDSI

In general, an NDSI threshold value of 0.4 has been the consensus value for making SCA maps, first suggested by Dozier (1989) based on visual inspection of imagery. However recent research has demonstrated that the selection of a NDSI threshold for SCA depends on many factors. Threshold values for SCA based on the NDSI may be chosen by automated methods such as discussed in Yin et al., (2013) to optimize the threshold to the imagery and landscape conditions. The heritage MODIS SCA algorithm, used in the MOD10\_L2 and MYD10\_L2 products, employed an NDSI threshold of 0.4 and an extended low range 0.1 – 0.4 NDSI range coupled with the NDVI to improve snow detection in dense snow covered vegetation (Klein, et al.; 1998, Riggs et al 2006). The NDSI as discussed so far has been used to map SCA as a binary map of snow on the landscape. However the NDSI can be used to estimate all viewable snow cover on the surface and track the onset and duration of snow cover on the landscape.

An estimation of fractional snow cover (FSC) over the landscape, or viewable fraction of snow on the landscape is a more useful measure of snow cover than is the binary SCA because FSC ranges from 0-100% and conveys information about the amount of snow visible on the landscape. Fractional snow cover is considered as the viewable fraction of snow in a pixel (Nolin, 2010), which may not be the actual areal extent of snow in a pixel. For example; the Canadian boreal forest in winter with a 100% surface cover of snow will have high NDSI values around 0.7 but will not be near 1.0 because of forest canopy, viewing and solar geometry. The NDSI is an index of the snow cover viewable on the landscape that can be interpreted as an estimate of FSC.

Various methods have been used to estimate FSC including; spectral mixture analysis (Rosenthal and Dozier, 1996; Painter et.al. 2009; Rittger et al. 2013) primarily for alpine landscapes; semi empirical modeling of snow reflectance (Metsämäki et al. 2005 and 2012) over the Scandinavian boreal zone; and regression of empirical relationship between a low resolution sensor and a higher resolution sensor such as MODIS with Landsat TM (Solomonson and Appel, 2004 and 2006) to estimate snow fraction based on the NDSI. Determination of FSC in the MODIS C5 algorithm is based on the regression relationship of NDSI to FSC developed from the empirical relationships found between MODIS (Terra and Aqua) and Landsat TM data (Solomonson and Appel, 2004 and 2006).

## **2.2 Algorithm Description (The Normalized Difference Snow Index (NDSI))**

The NDSI is a robust indicator of snow on the surface that has been used in various forms by many investigators since the late 1980s; primarily to generate SCA maps based on setting an NDSI threshold above which the surface is considered as 100% snow covered and below which the surface is considered not snow covered. The NDSI is a measure of the relative difference of reflectance between a VIS band and a SWIR band. The basic NDSI applicable to sensors with VIS and SWIR channels is;  $NDSI = (VIS - SWIR) / (VIS + SWIR)$

The VIIRS NDSI is:

$$NDSI = (I1 - I3) / (I1 + I3)$$

Where; I1 is VIIRS band I1, 0.64  $\mu\text{m}$ , and I3 is VIIRS band I3 1.61  $\mu\text{m}$ , both at 375 m resolution.



It is an index that indicates the presence of snow cover on the surface based on snow characteristics of high VIS reflectance and very low SWIR. If snow is present and viewable by a satellite then the NDSI will be in the theoretical range of -1.0 to 1.0, with a value of 0.0 or less indicating no snow. However, in practice the NDSI for snow ranges from 0.0 to 1.0. If snow is present and viewable by the sensor the NDSI will be  $> 0$ . An accepted global NDSI threshold value used has been 0.4, although many researchers have shown that better SCA maps can be made in specific situations for local or regional snow mapping if, for example, the NDSI is set for that situation with methods of threshold selection based on visual inspection/interpretation, empirical relationship or automated selection (Yin et al., 2013). In such cases the NDSI threshold setting may be as low as 0.1 for SCA determination.

The ability to detect snow cover is related to the difference in VIS and SWIR. The greater the VIS-SWIR difference the greater the NDSI. To illustrate the NDSI let us assume that snow VIS reflectance increases from 0.0 to 1.0 in increments of 0.1 and that the SWIR reflectance remains constant at 0.10 (solid line in Fig. 3). A SWIR reflectance of 0.10 from snow is reasonable for a snow covered surface with minimal vegetation or other surface features based on reflectance plots in the literature and extensive visual interpretation experience of analysis of MODIS imagery. As the visible reflectance increases the NDSI increases as shown by the solid black line in Fig. 3.

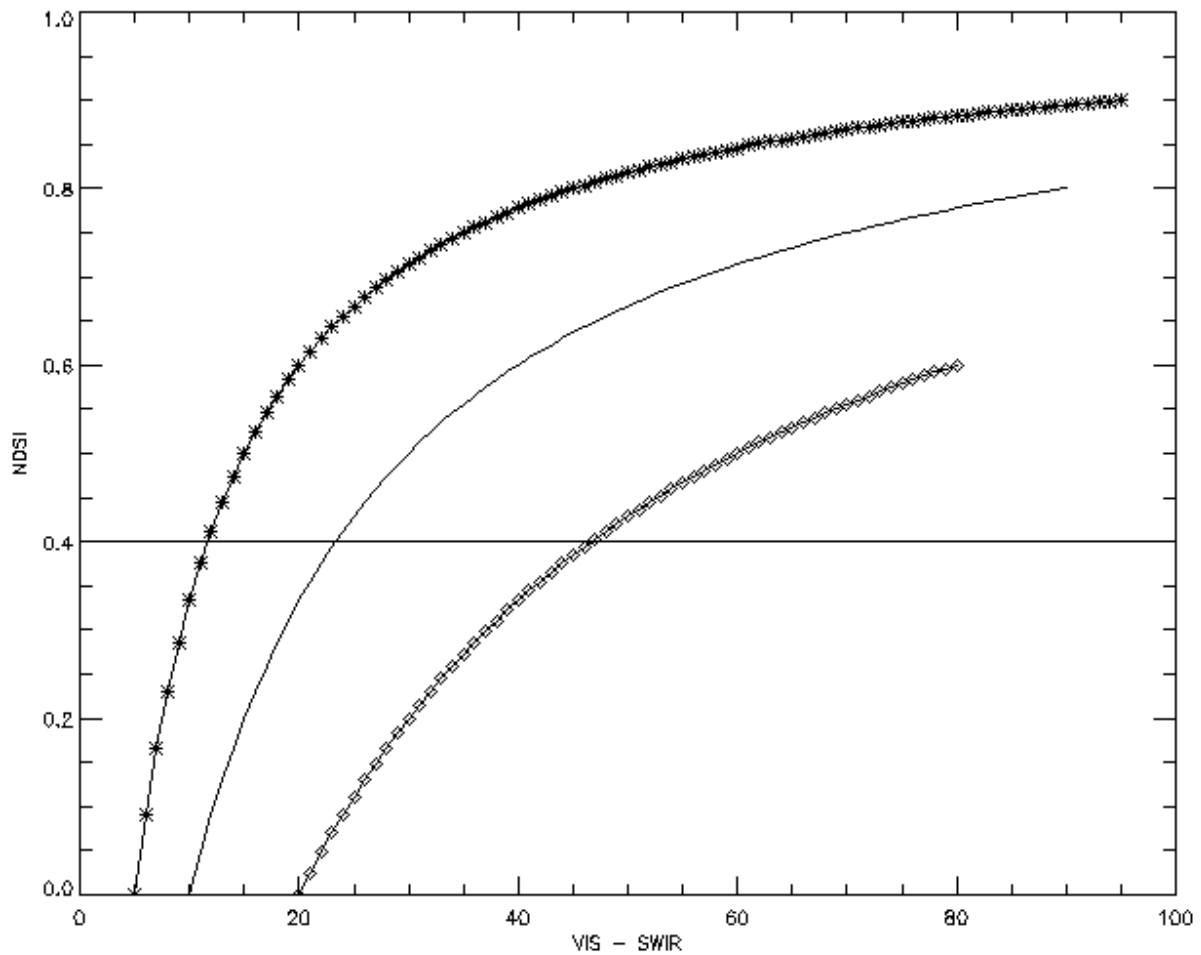


Figure 3. NDSI plots. Plotted are the NDSI values for three conditions. The solid line is the NDSI with the VIS reflectance increasing from 0 to 100% in increments of 1% while the SWIR reflectance is constant at 10%. The asterisks line is VIS reflectance increasing from 0 to 100% in increments of 1% while the SWIR reflectance is constant at 5%. The diamonds line is VIS reflectance increasing from 0 to 100% in increments of 1% while the SWIR reflectance is constant at 20%.

The NDSI is plotted against the VIS to SWIR difference to show change in NDSI as the difference between VIS and SWIR increases in Figure 3. As the VIS reflectance increases the difference between VIS and SWIR increases, thus the NDSI increases reaching a maximum NDSI of 0.81 (Fig. 3). The asterisk line in Fig. 3 with snow at lower SWIR reflectance of 5% with VIS increasing from 0 to 100% has a larger VIS to SWIR difference and the NDSI increases more rapidly before slowing and reaching a horizontal asymptote at ~ 0.90 NDSI. Conversely, the diamond line in Fig. 3 with snow at higher SWIR reflectance 20% the NDSI curve increases relatively slowly and reaches an asymptote at ~ 0.67 NDIS. As shown the greater the VIS-SWIR difference the greater the NDSI. This difference increases the certainty of snow cover detection. As the VIS - SWIR difference decreases so does the NDSI as well as the

range of NDSI values. Thus with a lower difference the certainty of snow cover detection decreases.

Mishra et al. (2009) investigated the range of NDSI value of snow in the Himalayan region relative to subpixel snow modeling and found that NDSI can range from 0.04 to 0.92 with increasing amounts of snow cover. They also found that different snow fractions in a pixel may have the same NDSI value due to percentages of other components in reflectance from a pixel.

Studies of the interannual variability of snow cover depletion curves have found that the NDSI can provide more information than a binary SCA (e.g., Kolberg and Gottschalk, 2010). The NDSI has also been used in neural network research of snow cover mapping because of more information content than binary SCA e.g. Dobрева and Klein (2011). This is in part because the use of an NDSI threshold to make a binary SCA ignores the ability to map snow cover at lower NDSI values. If an NDSI threshold for snow cover is set at 0.4, that threshold line is drawn in Fig. 3, then any snow cover with lower value will be excluded from the SCA map, which could be a significant amount of snow depending on conditions. Some researchers have noted the ability to correctly detect snow below the 0.4 NDSI threshold (Jain et al., 2008; Hassan et al., 2012; Lin et al. (2012). Also, NDSI from higher spatial resolution sensors has also been used with great success to delineate glaciers (Racoviteanu et al., 2008), and to accurately detect glacier ice in complex shadowed terrain (Burns and Nolin, 2014). It is possible to make more accurate snow cover maps with higher resolution sensors, i.e. VIIRS at 375 m compared to the MODIS at 500 m resolution albeit with a small but notable increase in accuracy.

The NDSI varies across a snow covered landscape in relation to the landscape and viewing conditions, e.g. see Mishra et al. (2009). Diversity of NDSI across the landscape is found in all MODIS and VIIRS imagery. The VIIRS acquisition of 5 December 2014, 1945 UTC (Fig. 4) is used to demonstrate the diversity of snow cover across a landscape of snow covered plains, boreal forests and mountains.

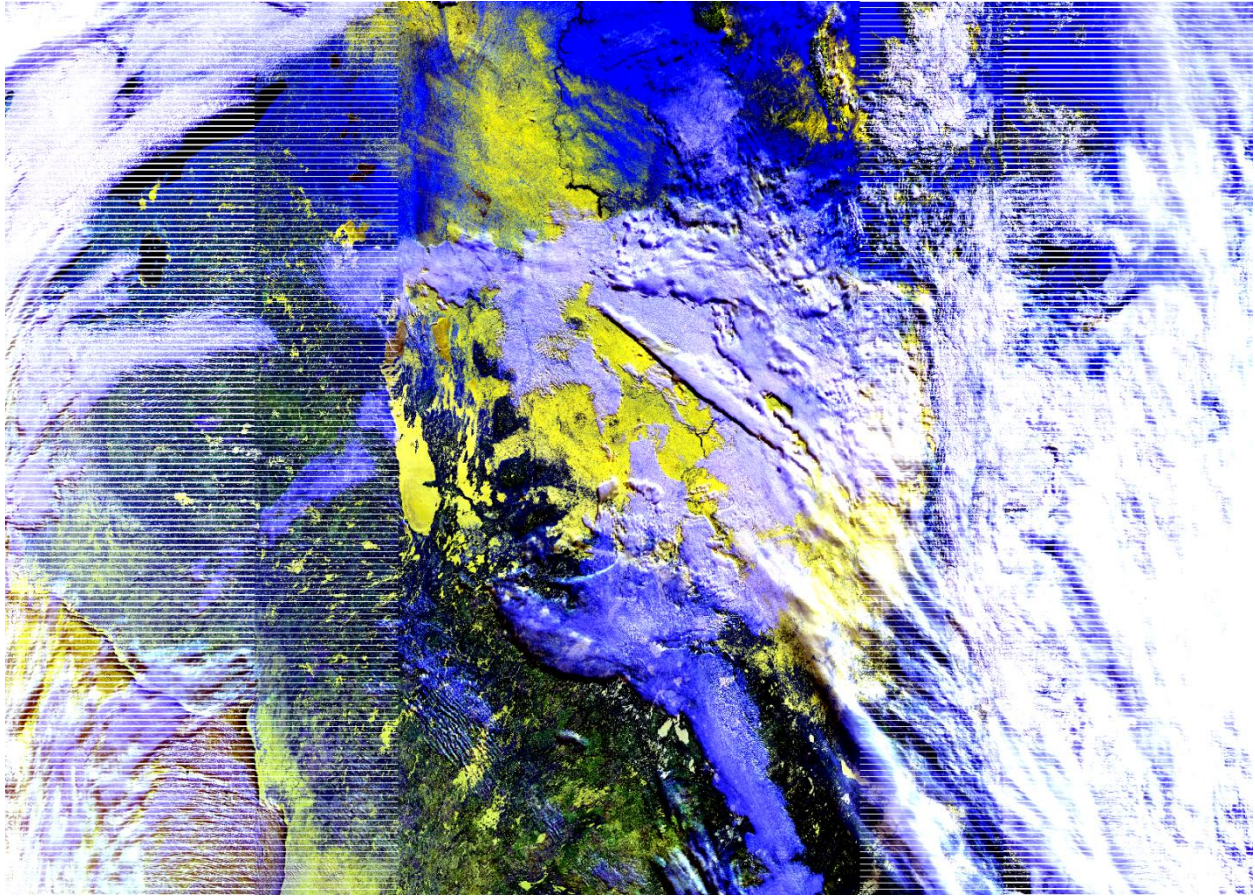


Figure 4. VIIRS false color image of bands I1, I2, I3 (RGB) TOA reflectance from the NASA Land SIPS NPP\_VIAE\_L1.A2014339.1945.P1\_03001.\* product. In this band combination snow cover appears in shades of yellow on plains and snow covered lakes, and yellowish to dark blue in boreal forests; snow free surfaces appear in shades of bright blue, and clouds appear in white to bluish-white depending on the type or thickness of cloud cover. South is at top of image, snow covered Northern Plains top center, Lake Winnipeg left center of image, Hudson Bay in lower left, Lake Superior in upper left. The white stripes on either side of the image is the bowtie trim.

The resulting NDSI image is shown in Fig. 5 with NDSI in shades of grey. Visually the NDSI values in Fig. 5 correspond to the observed snow cover across all the landscape surface features ( Fig. 4); negative NDSI values appear in black; areas of “no snow”, and the highest NDSI values are shown in white. Snow cover has higher NDSI values than other features and appears as light grey to white shades. Snow cover on the plains and frozen lakes has the highest NDSI values. Snow covered forests have a lower range of NDSI values, mid grey shades which is relatively strong indicator of snow. In this image, clouds, oceans and bowtie trim are masked and shown in dark grey, with NDSI set to 0.0.

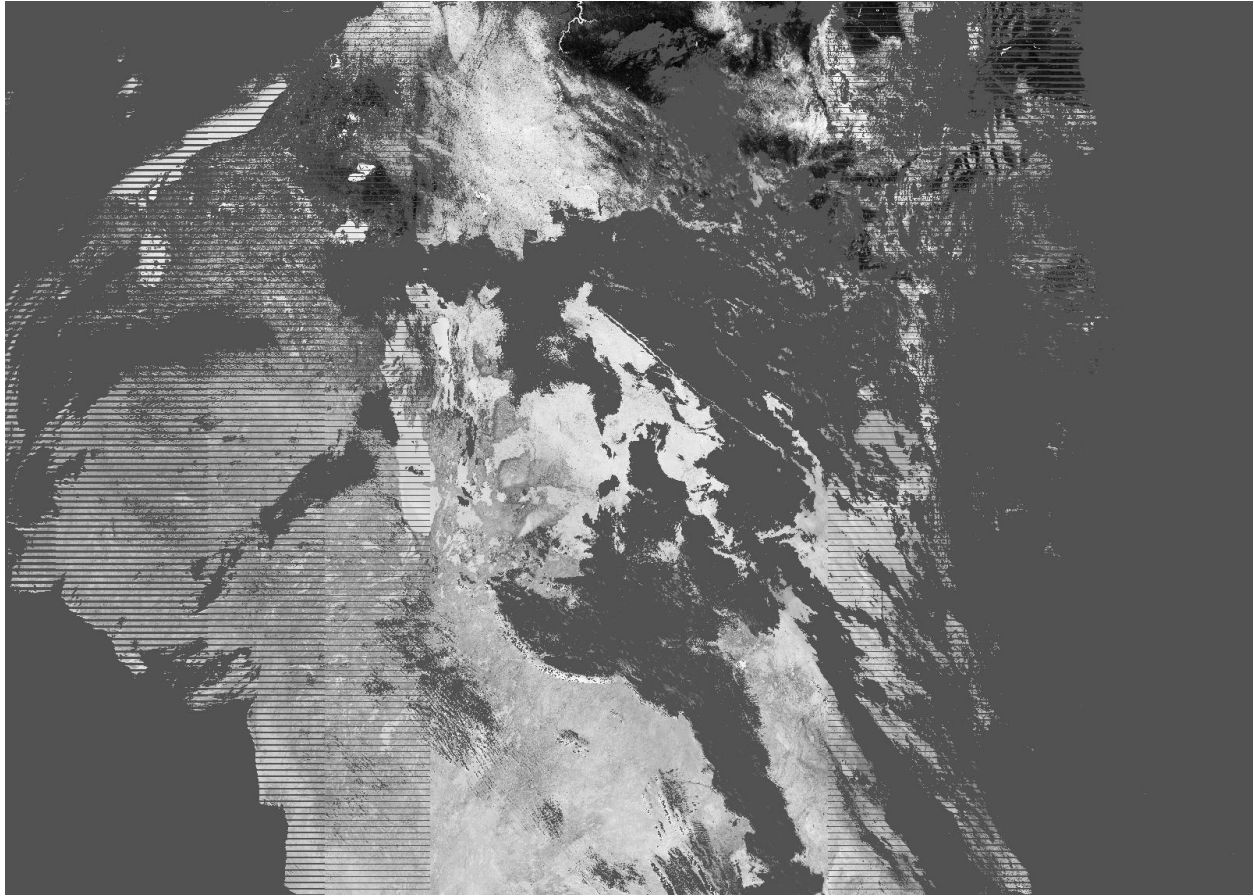


Figure 5. NDSI image for VIIRS image NPP\_VIAE\_L1.A2014339.1945.P1\_03001. (Fig.4). Clouds, oceans and bowtie trim have been set to NDSI=0.0 and are shown in dark grey. Non-snow surfaces are shown in black with  $\text{NDSI} < 0.0$ . Snow cover NDSI values range from  $> 0.0$  to 1.0 and are shown in shades from light grey to white.

The histogram of NDSI values (Fig. 6) for in the scene shown in Fig. 4 has a tail in the distribution of NDSI values of less than about 0.3. That low range tail of NDSI values corresponds to situations where viewable reflectance from snow cover is low due to forest canopy, terrain shading, cloud shadows, thin or sparse snow cover in a pixel, or perhaps is a non-snow feature that has a positive NDSI value. Thus the region in the range of  $0.0 < \text{NDSI} \leq 0.30$ , is where snow cover can be detected but with increased uncertainty in snow cover detection.

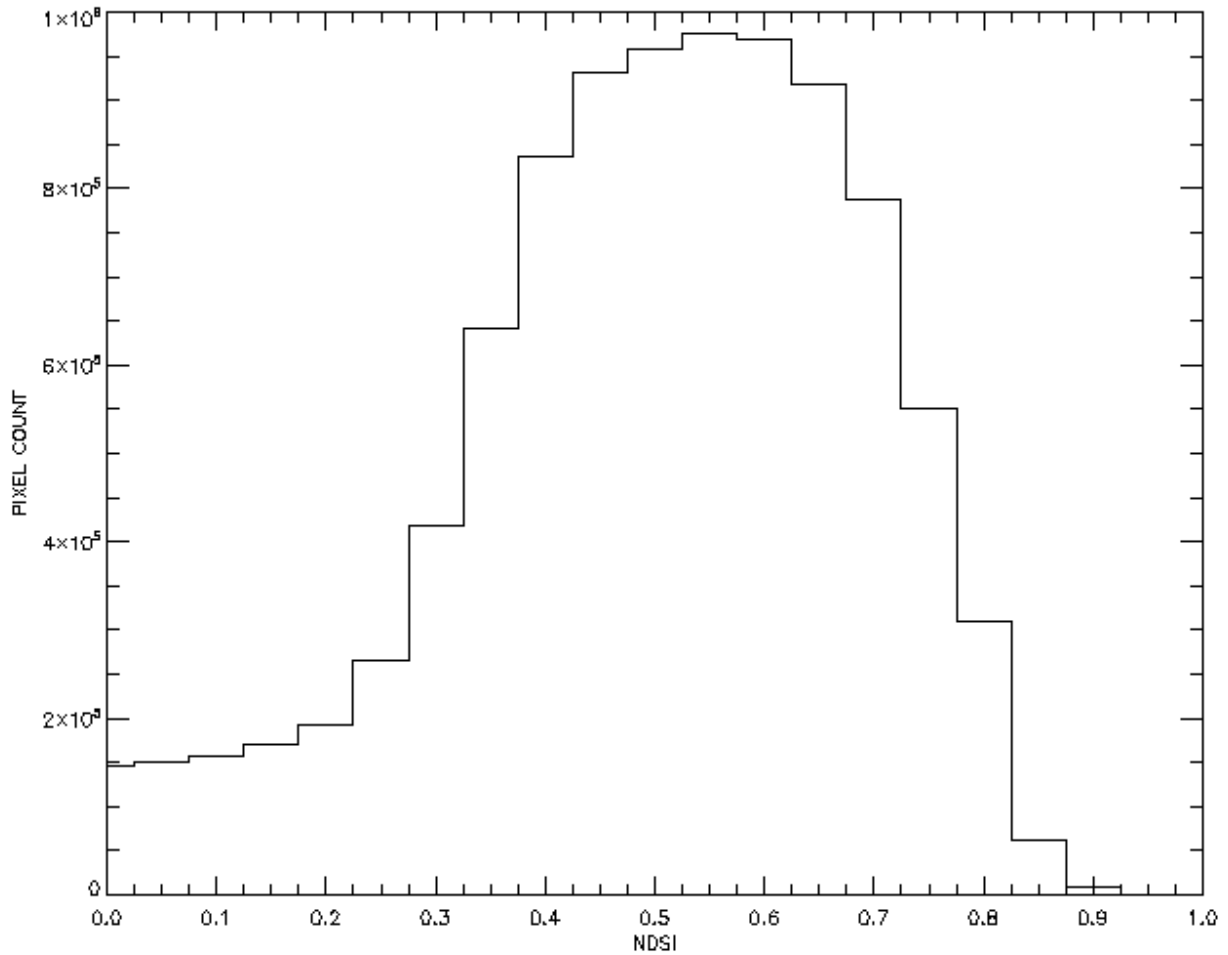


Figure 6. NDSI histogram for the NPP\_VIAE\_L1.A2014339.1945.P1\_03001 image (Fig. 4). The histogram was calculated with NDSI bin size of 0.05.

The following discussion demonstrates that the snow cover map obtained from using the full range of NDSI is more accurate than using the standard NDSI threshold of 0.4 to make a SCA map. Using an NDSI threshold of 0.4 the SCA map shown in Figure 7 is created and in that map 70% of the land area is covered by snow (shown in white). However, using that NDSI threshold blocks from detection a significant extent of snow in some regions, such as in the forests and along the edges of plains and mountain snow cover. Lowering the NDSI threshold to  $> 0.01$  increased SCA extent, the areas shown in red, by 20%. Detecting snow cover over the entire range  $0.0 > \text{NDSI} \leq 1.0$  results in a more accurate representation of snow cover across the landscape, especially in the forest to the north of Lake Superior and at edges of snow covered regions, with 90% of the visible land area being mapped with snow cover.

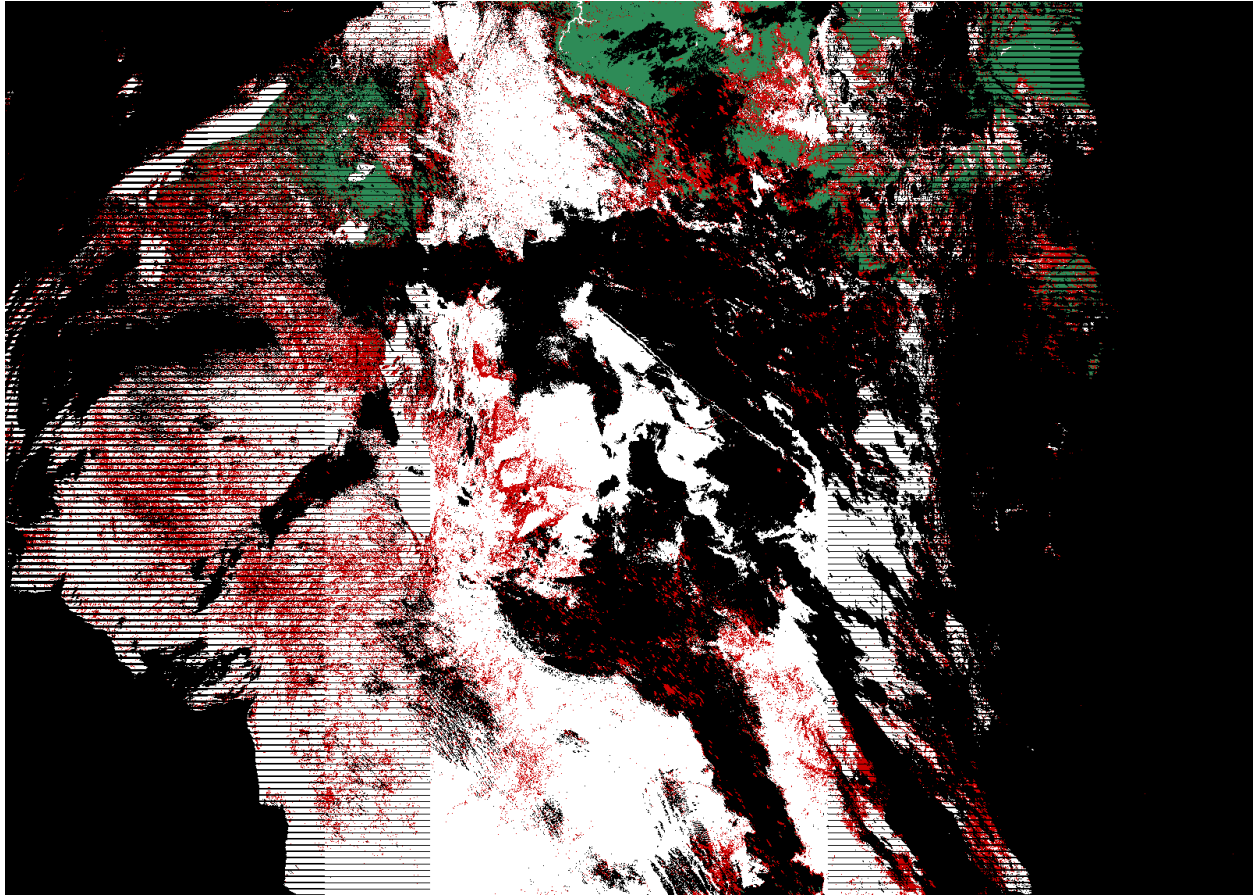


Figure 7. Snow cover area (SCA) map for NPP\_VIAE\_L1.A2014339.1945.P1\_03001 image using the NDSI threshold technique. SCA corresponding to  $NDSI \geq 0.4$  in white. SCA corresponding to  $0.0 < NDSI < 0.4$  in red. Snow free land is shown in green. Clouds, oceans and bowtie trim in black. . Visual analysis of this SCA map as compared to a visible image indicates that the accuracy of the SCA map is greater when the full range of NDSI is used as compared to using the 0.4 threshold.

A more accurate snow map and increased information regarding snow cover can be conveyed in the NDSI data so the VIIRS snow cover algorithm and product will deviate from the heritage MODIS C5 snow algorithm and data product. Note that the MODIS C6 snow algorithm does not use the 0.4 threshold, but uses the entire NDSI range 0.0 – 1.0 to map snow. Motivating reasons to deviate from the heritage MODIS C5 algorithm and products are to increase accuracy of snow cover detection and increase a user's flexibility in using the data. The NDSI is used in both the heritage MODIS C5 algorithm and the VIIRS algorithm so that the continuity of snow cover detection is maintained between instruments albeit the algorithm implementation and data product content are different. Those differences are only relevant to the MODIS C5 data collection because the MODIS C6 algorithm and data product are very similar to the VIIRS algorithm. The MODIS C6 and VIIRS algorithms were developed together, leveraging analysis and evaluation from both to make nearly identical algorithms. Differences between the MODIS

C6 and the VIIRS algorithms are related to the physical differences between MODIS and VIIRS sensors spatial resolution and band location and width.

The 0.4 NDSI threshold was selected as a global threshold for making SCA maps however, recent research discussed above demonstrates that an NDSI threshold selection should be left to the user. A user can make their own SCA map using the NDSI snow cover or NDSI data arrays in the product and setting the NDSI threshold appropriate for their usage. A SCA data array will not be included in the VIIRS snow cover product. In the MODIS C5 heritage SCA algorithm the NDSI threshold for binary snow cover was set at 0.4 which had the effect of blocking possible snow cover with lower NDSI values, as shown by the horizontal line in Fig. 8. The heritage MODIS C5 SCA algorithm also includes an extended low NDSI range of 0.1 – 0.4 NDSI coupled with the NDVI to improve snow detection in dense snow covered vegetation (Klein et al. 1998; Riggs et al 2006).

The heritage MODIS C5 FSC was calculated using the NDSI in a regression equation (Fig. 8). That regression equation was determined by empirical relationship of a MODIS 500 m pixel to the estimated snow in the corresponding Landsat TM 30 m pixels (Solomonson and Appel, 2004 and 2006) to estimate the MODIS snow fraction based on the NDSI. The VIIRS has higher spatial resolution, 375 m, as compared to MODIS, and band widths and locations that are different from MODIS. That FSC regression relationship reaches a maximum of 100% FSC at an NDSI of approximately 0.7 and is held at that maximum for all higher NDSI values (Fig. 8) thus blocks extracting information about snow cover in the NDSI range of 0.7 – 1.0. The MODIS C6 snow cover data product does not include the FSC data array.



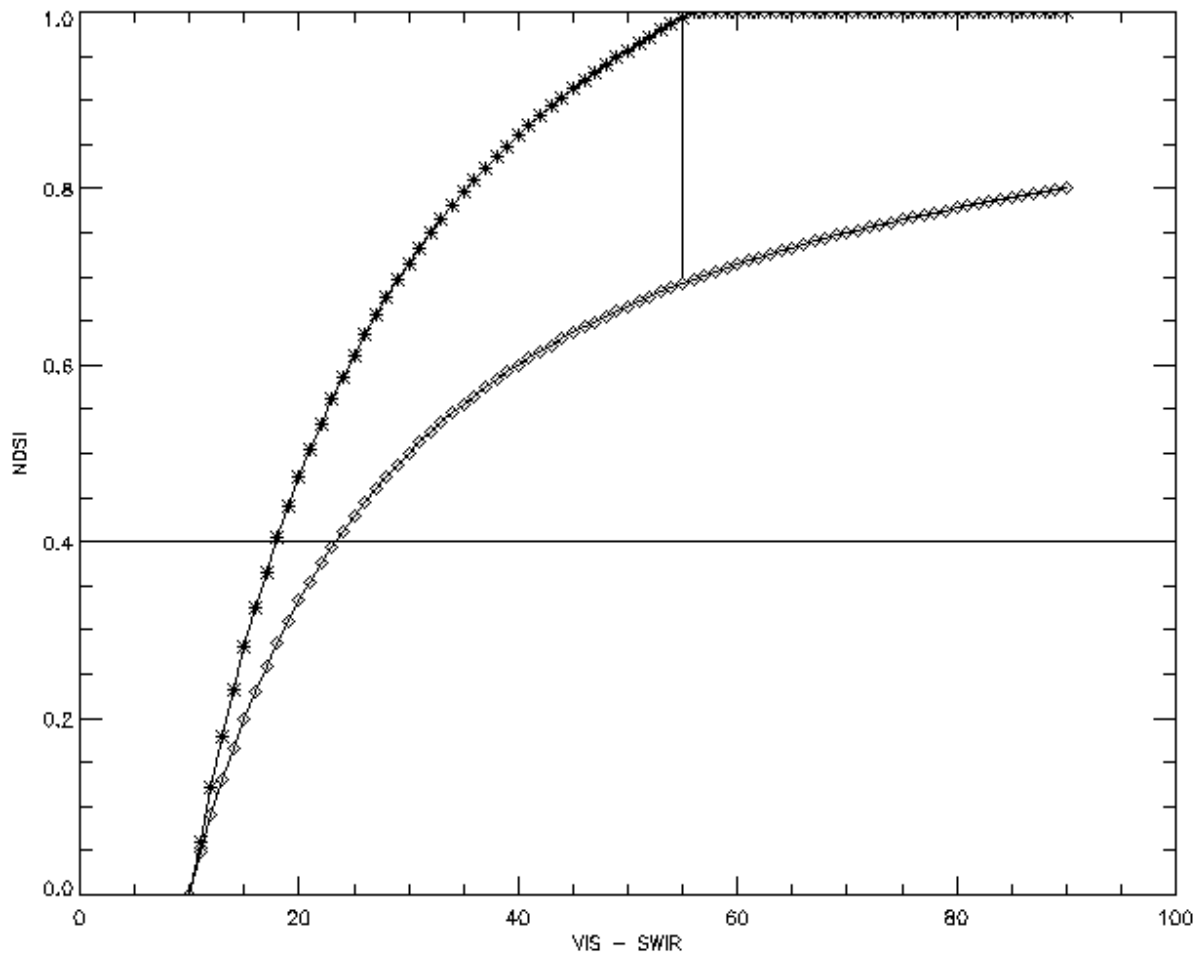


Figure 8. The MODIS Terra C5 SCA and FSC relationship. The NDSI was calculated by incrementing VIS reflectance from 0 to 100% in 1% increments while holding SWIR reflectance constant at 5%, the diamond line. The MODIS SCA was determined by NDSI threshold set at 0.4, horizontal line at 0.4 NDSI, snow above that line, not snow below. The MODIS FSC (asterisks line) was calculated as  $FSC = -0.01 + (1.45 * NDSI)$ . FSC reaches maximum value of 1.0 at  $NDSI = 0.7$  shown by black vertical line.

The VIIRS snow cover product will contain the NDSI snow map and NDSI data values for all land and inland water body pixels in the scene. Including the NDSI data for all features will allow user options to create their own snow cover map using the NDSI or a combination of the NDSI, NDSI snow cover and QA bit flags. MODIS Collection 6 snow cover products include the NDSI snow cover and NDSI data arrays. When MODIS Collection 6 reprocessing is complete there will be a NDSI data set spanning the MODIS and VIIRS operational missions.

### 2.2.1 Algorithm Limitations

Though the NDSI is a robust technique for snow detection it does have limitations. The limitations are discussed in Section 3.2 regarding mask and data screens applied and in Section 4.0 as uncertainty and error in snow detection. Two classes of error are omission errors, missing snow when snow is present, and commission errors, detecting non-snow features as snow. Snow

omission error is generally uncommon. Commission error is the most common snow detection error and may occur over the full range of NDSI values ( $0.0 < \text{NDSI} \leq 1.0$ ). To decrease snow commission errors, data screens and thresholds are applied to snow detections in the algorithm to detect spectral features or characteristics that are not characteristic of snow; estimated surface temperature linked with geoid height is applied as a screen. Snow detections that fail any of those screens or thresholds will have a QA bit flag set to indicate that the snow detection is reversed or to flag uncertain snow detection. The screens and thresholds are described in Sec. 3.2.

Clouds are the greatest limitation and source of uncertainty in VIIRS snow cover detection. The snow cover algorithm uses the VIIRS Cloud Mask Intermediate Products (CMIP) to mask clouds as described in Section 3.2. Accurate detection of clouds over snow is a challenging problem for which the CMIP algorithm generally gives a correct result but there is notable snow/cloud confusion, wherein snow covered is detected as certain cloud, or clouds are not detected as clouds that can exist in the CMIP. That confusion then can cause errors of omission or commission, or increased uncertainty in the snow detection algorithm. This version of the snow cover algorithm does not attempt to resolve snow/cloud discrimination errors; it simply uses the CMIP as the cloud mask. Along with the University of Wisconsin cloud masking group, we are investigating ways to improve snow cloud discrimination.

### **2.2.2 Algorithm Flow**

The algorithm is run for all land and inland water pixels in daylight in a swath without restrictions, then data screens and masks are applied. The NDSI is calculated for all land and inland water pixels in daylight in a swath then data screens are applied to snow detections or to all pixels depending. QA bit flags may be set, then the basic QA value is determined, the cloud mask is then applied to all data arrays except the NDSI data, and finally the data arrays are output. This algorithm flow is used so that the algorithm is applied under all conditions then the results are then screened and flagged so that users can inspect the QA bit flags to determine if the result for a pixel is usable in their research or application.

## **2.3 Product Description**

The VIIRS Level-2 Snow Cover Data Product, ESDT name VNP10, will have the following data arrays, NDSI\_snow\_cover, basic QA, QA bit flags, and NDSI data with local attributes describing the data, and global metadata in the file to support archiving and use of the product.

### NDSI\_snow\_cover

The NDSI snow cover data array is the snow cover extent map generated by the algorithm. Snow cover is represented by NDSI values in the range of 0 – 100, from no snow cover to total snow cover in a pixel. For all pixels that were detected as snow the data screens were applied and the snow detection may have been reversed to not snow or flagged as uncertain snow

detection. Algorithm QA bit flags are set if a snow detection was reversed or flagged as uncertain by one or more data screens applied in the algorithm. To give a complete view of viewing conditions in the scene the cloud mask, ocean mask, and night mask, if needed, are overlaid on the NDSI snow cover data. Local attributes describing the data are included for the data array.

Basic QA

A general quality value is given for both pixels processed for snow cover and pixels not processed, e.g. oceans have a masked value. This is a basic quality value use to indicate quality ranging from best to poor to provide a user with a convenient value for initial quality assessment of the data. Local attributes describing the data are included for the data array.

QA bit flags

Algorithm specific bit flags are set in this data array for the data screens applied in the algorithm. Multiple bit flags may be set. Local attributes describing the data, i.e. each bit flag, are included for the data array.

NDSI

The calculated NDSI values for all land and inland water pixels in the swath are in this data array. Data is in scaled format. Local attributes give information on how to un-scale the data. The cloud mask is not overlaid on the NDSI data.

**Table 1: Summary of land snow cover products produced at the Land SIPS**

<b>Products</b>	<b>ESDT</b>	<b>Description</b>
<b>Snow Cover (L2 Daily Swath product)</b>	VNP10	VIIRS/NPP Snow Cover 5-Min Swath 375 m
<b>Snow Cover (L2G Daily Tiled products)</b>	VNP10L2G	VIIRS/NPP Snow Cover Map Daily L2G Global DDR 375 m SIN Grid Day.

<b>Snow Cover (L3 Tiled products)</b>	VNP10A1	VIIRS/NPP Daily Snow Cover 375 m SIN Grid
	VNP10A2	VIIRS/NPP 8-Day Snow Cover 375 m SIN Grid
<b>Snow Cover (L3 CMG Products)</b>	VNP10C1	VIIRS/NPP Daily Snow Cover L3 Global DDR 0.05°x0.05° grid CMG

### 3.0 PRODUCT INPUTS

The Land PEATE or Land SIPS IDPS versions of the VIIRS input products have been used for algorithm development and evaluation. The NASA VIIRS products will be used as input when Land SIPS begins operational production of those products. Input ESDTs and data arrays (the bit flag used if a bit flag array) are listed in Table 2.

ESDT	Data array(s)	Nominal spatial resolution	Descriptor
NPP_VIAE_L1	Reflectance_I1	375 m	TOA
	QF1_VIIRSIBANDSDR_I1		Poor quality flag
	Reflectance_I2	375 m	
	QF1_VIIRSIBANDSDR_I2		Poor quality flag
	Reflectance_I3	375 m	TOA
	QF1_VIIRSIBANDSDR_I3		Poor quality flag
	BrightnessTemperature_I5	375 m	TOA
	QF1_VIIRSIBANDSDR_I5		Poor quality flag
NPP_VMAE_L1	Reflectance_M4	750 m	TOA
	QF1_VIIRSMBANDSDR_M4		Poor quality flag
	SolarZenithAngle	750 m	Solar zenith angle
NPP_IMFT_L1	Height	375 m	Terrain height
NPP_CMIP_L2	QF1_VIIRSCMIP (bits 2-3)	750 m	Cloud mask confidence
	QF2_VIIRSCMIP (bits 0-2)	750 m	Land/water mask

Table 2. VIIRS data product inputs to VNP10\_L2 algorithm. The ESDT and data array name(s) and bit flag(s) if a bit flag array is listed.

### 3.1 Spectral Bands

VIIRS VIS, SWIR and thermal bands are used as input. Input ESDTs and spectral bands are listed in Table 3.

ESDT	Data array	wavelength	Nominal spatial resolution
NPP_VIAE_L1	Reflectance_I1	0.640 $\mu\text{m}$	375 m
	Reflectance_I2	0.865 $\mu\text{m}$	375 m
	Reflectance_I3	1.61 $\mu\text{m}$	375 m
	BrightnessTemperature_I5	11.450 $\mu\text{m}$	375 m
NPP_VMAE_L1	Reflectance_M4	0.555 $\mu\text{m}$	750 m

Table 3. VIIRS spectral band inputs to VNP10\_L2 algorithm.

### 3.2 Masks, Thresholds and Ancillary Data

Several data screens, masks and thresholds are applied in the algorithm to mask clouds, flag uncertain snow detections, to reverse possible snow commission errors and set QA bit flags. Data screens, masks and thresholds used are created within the algorithm with data read from the VIIRS input data products. No ancillary data are used in the algorithm. Data screens and masks used are described below.

#### Land/Water Mask

The land/water mask is currently read from the IDPS CMIP product (NPP\_CMIP\_L2). When the NASA VIIRS version of the land/water mask based on the heritage MODIS land/water mask becomes available it will be used in the algorithm because of its heritage. It has more classes and better accuracy than the CMIP land/water mask. The land/water mask is used to mask oceans and to process inland water bodies. The VIIRS snow cover algorithm performs snow/ice detection on inland waters. The inland water mask is stored as a bit flag in the QA bit flag data array so that it can be used to extract just the inland waters data or mask inland waters depending on a user's need.

#### Cloud Mask

Discrimination of cloud from snow is very challenging because some types of clouds and snow can have very similar reflectance characteristics and NDSI values. The CMIP cloud confidence flag is used in the snow cover algorithm to mask clouds. If the cloud confidence flag reports certain cloud for a pixel that pixel is masked as cloud. If a pixel is certain clear or probably clear

or probably cloud, the pixel is processed as a clear view of the surface. The CMIP is gridded from its 750 m resolution to 375 m resolution using nearest neighbor technique.

The CMIP is accurate in cloud detection in most situations; however there are some persistent cloud/snow confusion problems that appear in the snow cover product. Some discussion of uncertainty in cloud detection is presented in Sec. 4.0. (Note: when the NASA version of the cloud mask product becomes available it will replace the IDPS CMIP product as the cloud mask input product.)

### Night Mask

The algorithm is not applied to pixels that are in darkness as determined by the solar zenith angle. A pixel is flagged as night if the solar zenith angle is  $\geq 85$  degrees. Solar zenith data is read from the NPP\_VMAE\_L1 product.

The purpose of data screens is to detect spectral features or characteristics that are unlike snow or are uncertain, i.e. weak indicator of snow. Snow commission errors, detection of snow free features as snow by the algorithm can be caused by the feature having an NDSI value in the  $0.0 > \text{NDSI} \leq 1.0$  range. Snow always has an  $\text{NDSI} > 0$ ; however, not all features with  $\text{NDSI} > 0$  are snow. To alleviate snow commission errors and to flag uncertain snow detections several screens and thresholds based on spectral features, and a combination of surface height and surface temperature are applied. The screens are applied to every pixel that was detected with snow cover; if a pixel fails one or more of the screens, it may be reversed to a non-snow result and QA bit flag(s) set or the snow detection may be flagged as uncertain. All the screens are applied to a pixel so several QA flags may be set for each pixel. A user can use those QA bit flags to find where and why snow pixels were changed to not snow and find where snow detections are uncertain.

### Low Visible Reflectance Screen

The algorithm is reflectance based, thus it depends on there being enough reflectance from the surface, any surface, in the VIS and SWIR bands, and a difference in amount of reflectance between VIS and SWIR bands, for the NDSI calculation to give a reliable result. Low reflectance can be associated with high solar zenith angle, topographic shading, cloud shadows or an intrinsic property of the surface. The algorithm is pushed to its limits for snow detection globally balanced against not running the algorithm in low reflectance situations. However if reflectance is too low, that is a no decision situation, and snow detection is not done. A no decision result avoids possible snow commission errors in low reflectance conditions.

Specification of what is the minimum amount of VIS reflectance is based on the possibility of omission and commission errors occurring in relation to a lack of reflectance from a surface. Published snow spectra curves (cited in Sec. 2.1) and analysis of spectral plots from MODIS and VIIRS data have been used to empirically determine a reasonable lower limit of reflectance to apply in the algorithm. The lower VIS reflectance limit is the same as used in the MODIS C6

snow cover algorithm. If VIS reflectance from the surface is  $< 0.10$  in band I2 or  $< 0.11$  in band M4 the algorithm reverses snow detection to a no decision result.

### Low NDSI Screen

The difference between VIS and SWIR reflectance for snow determines the NDSI value. As shown in Fig. 3 small differences in VIS – SWIR have low NDSI values and large differences have large NDSI values. In addition, the NDSI value increases rapidly with the VIS – SWIR difference, and is dependent on the magnitude of VIS and NIR reflectance. A reflectance curve across the VIS and SWIR parts of the spectrum from any surface, that lacks any well defined features, that is a nearly “flat” reflectance plot, may have a very small difference between VIS and SWIR reflectance that gives a small positive NDSI value thus; very low NDSI values are interpreted as highly uncertain snow detection. Because of the uncertainty of snow detection from a pixel with a “flat” reflectance curve a low NDSI screen with a threshold of 0.1 is applied. An NDSI value  $< 0.1$  is set to 0.0 and a QA bit flag is set. The NDSI  $< 0.1$  threshold was set based on analysis of MODIS and VIIRS ‘flat’ reflectance situations across a variety of landscapes and viewing conditions.

### Decreasing Visible Reflectance Screen

Decreasing visible reflectance across VIIRS bands, in wavelength order, M4 to I1 to I2 is atypical of snow so a screen is applied for this situation. If a snow cover detection has this reflectance characteristic, the snow cover detection is not changed but a QA bit flag is set for this uncertain snow cover detection. This screen has not been implemented in the current version of the algorithm, further evaluation of results in more situations is needed.

### High SWIR Reflectance Screen

Snow typically has low SWIR reflectance, less than about 0.10, because it absorbs SWIR. Snow mixed with vegetation, or other features may have a higher SWIR caused by SWIR reflectance from vegetation, yet may have a relatively high NDSI value. There is a wide range of SWIR reflectance and NDSI values associated with snow cover in different land covers and viewing conditions. Some cloud types with some ice content and some surfaces, e.g. bright sand, can have both high VIS and SWIR with VIS greater than SWIR resulting in  $NDSI > 0.0$ . In those situations those features appear to be snow, however the amount of SWIR is atypical of snow. A high SWIR reflectance screen using two thresholds is applied to either flag snow detection as uncertain or reverse snow detection to not snow. The lower threshold setting is for  $0.25 < SWIR \leq 0.45$  which is indicative of an uncertain snow detection, possibly snow mixed with vegetation or some specular reflectance from snow cover, thus the snow detection is not changed but a QA bit flag is set to indicate uncertainty. The high threshold setting is  $SWIR > 0.45$ , which is atypical of snow, in this case the snow detection is set to 0.0 and a QA bit flag is set to indicate reason for the snow reversal. This latter situation has been observed to occur with clouds with some ice content that were not detected as certain cloud by the CMIP algorithm.

## Surface Brightness Temperature and Surface Height Screen

The lesson learned with MODIS snow cover detection in C5 was that reversing a snow cover detection based on temperature alone could have detrimental results in some snow cover situations. However, the use of a surface temperature screen has been very effective at alleviating nearly all surface related snow commission errors on warm surfaces in the MOD10\_L2 C5 and VIIRS VSCM snow cover products however it has a drawback to global usage. The surface temperature screen in MOD10\_L2 C5 causes reversal of snow cover detection to no snow on some mountain ranges during spring and summer seasons (<http://modis-snow-ice.gsfc.nasa.gov/?c=collection6>). On mountains, mixed pixels with snow, rocks and/or vegetation can have an estimated surface temperature greater than 0° C because of the contribution of non-snow features to the sensed surface temperature. Assuming possible contributions of non snow features in a pixel the surface temperature screen was set at 283K. The MOD10\_L2 C5 algorithm reversed snow detection to snow free land if the sensed temperature was above that threshold. Mixed pixel, which included snow, had estimated surface temperatures above that threshold in the warm season. Reversal of snow detection by that screen resulted in significant snow commission errors on the Sierra Nevada range in spring and summer. The most detrimental impact of the screen was to eliminate snow cover when it still existed. Details concerning that problem and its impact through a spring and summer are presented on the MODIS snow/ice project website <http://modis-snow-ice.gsfc.nasa.gov/?c=collection6>

There are two factors to consider for using the surface temperature screen: 1) it is effective at alleviating snow commission errors on warm features that have a positive NDSI but are not snow that other screens fail to detect as not snow, and 2) it may cause omission errors on mountain ranges with snow cover in warm seasons. Linking the surface temperature screen with surface height applies the screen where it can be most effective and does not apply it on higher elevations of mountain ranges where it can cause significant snow omission errors. The surface temperature screen is linked with the surface height and only applied at surface heights < 1300 m. Surface temperature is estimated as the brightness temperature of band I5 and the surface temperature threshold is set at 281 K as too warm for snow. If a snow detection is at a height < 1300 m and too warm it is reversed to not snow and a QA bit flag is set. If snow detection is at ≥ 1300 m and too warm, i.e. above the surface temperature screen threshold, the QA bit flag is set to indicate warm snow detection.

The effectiveness of the surface temperature screen linked with surface height is shown in Fig. 9 where snow commission errors on cloud-shadowed Brazil forests are changed to not snow.



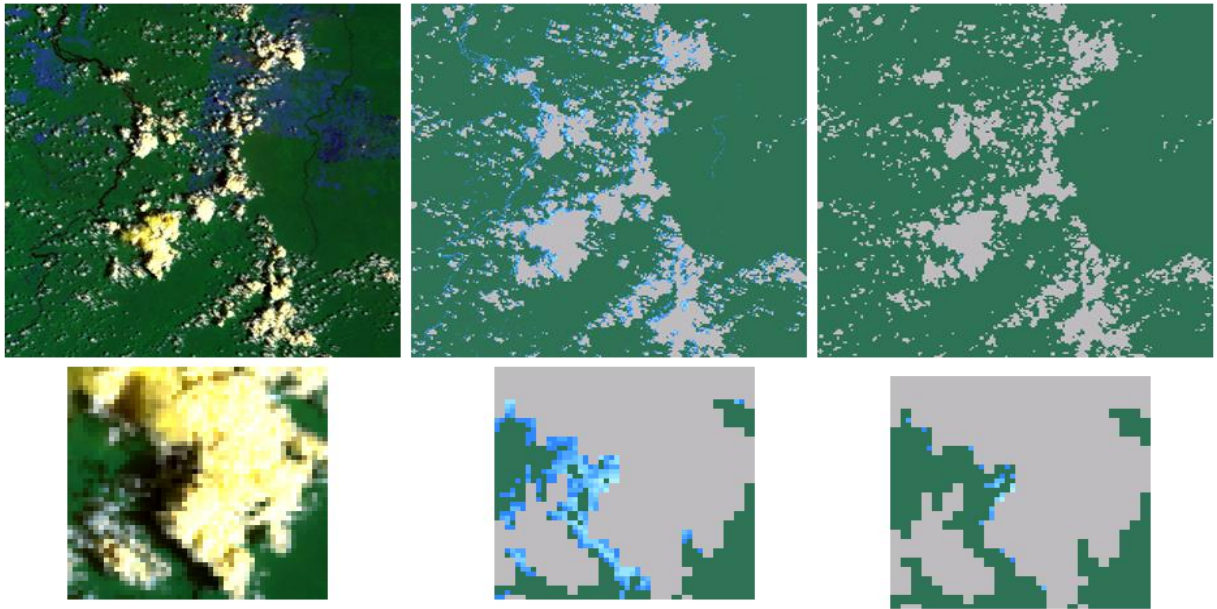


Figure 9. Image of southeastern Brazil from VIIRS swath of 2014255.1720.PI\_03001. False color image of I1, I2, I3 in top left image, zoom of cloud shadow detail in bottom left image. VIIRS NDSI snow cover output without the surface temperature screen in middle images, top and bottom zoom showing the snow commission errors associated with cloud shadowed land and fringes of cloud. VIIRS NDSI snow cover output with the surface temperature screen applied in right images top image and bottom zoom showing the effectiveness of alleviating snow commission errors. A few pixels of snow commission error remain at fringe of cloud, which have NDSI > 0.0 and are below the surface temperature threshold and not reversed by other screens.

### High Solar Zenith Screen

The highest potential accuracy of the VIIRS snow detection algorithm occurs where solar zenith angles are  $\leq 70^\circ$ . At solar zenith angles in the range of  $85^\circ$  to  $70^\circ$  the accuracy of the algorithm is lower; uncertainty in snow detection increases because of the low illumination in that viewing geometry. Low illumination in solar zenith angle range of  $70^\circ$  to  $85^\circ$  affects much of the Northern Hemisphere in the winter making it a challenge to detect snow. With lower illumination the amount of reflectance can be reduced, especially in snow covered boreal forests. Despite reduced illumination snow cover can be detected by the NDSI. Solar zenith mask for the swath shown in Figs. 4, 5 and 7 is shown in Fig. 10. Much of the snow covered landscape in this swath lies in the lesser-accuracy solar zenith range, the gray area in the mask, however snow cover (Figs. 5 and 7) is accurately detected in those illumination conditions. A QA bit flag is set for all pixels that have a solar zenith angle between  $70^\circ < \text{solar zenith angle} < 85^\circ$ . The purpose of this flag is to indicate possible increased uncertainty in the algorithm result.

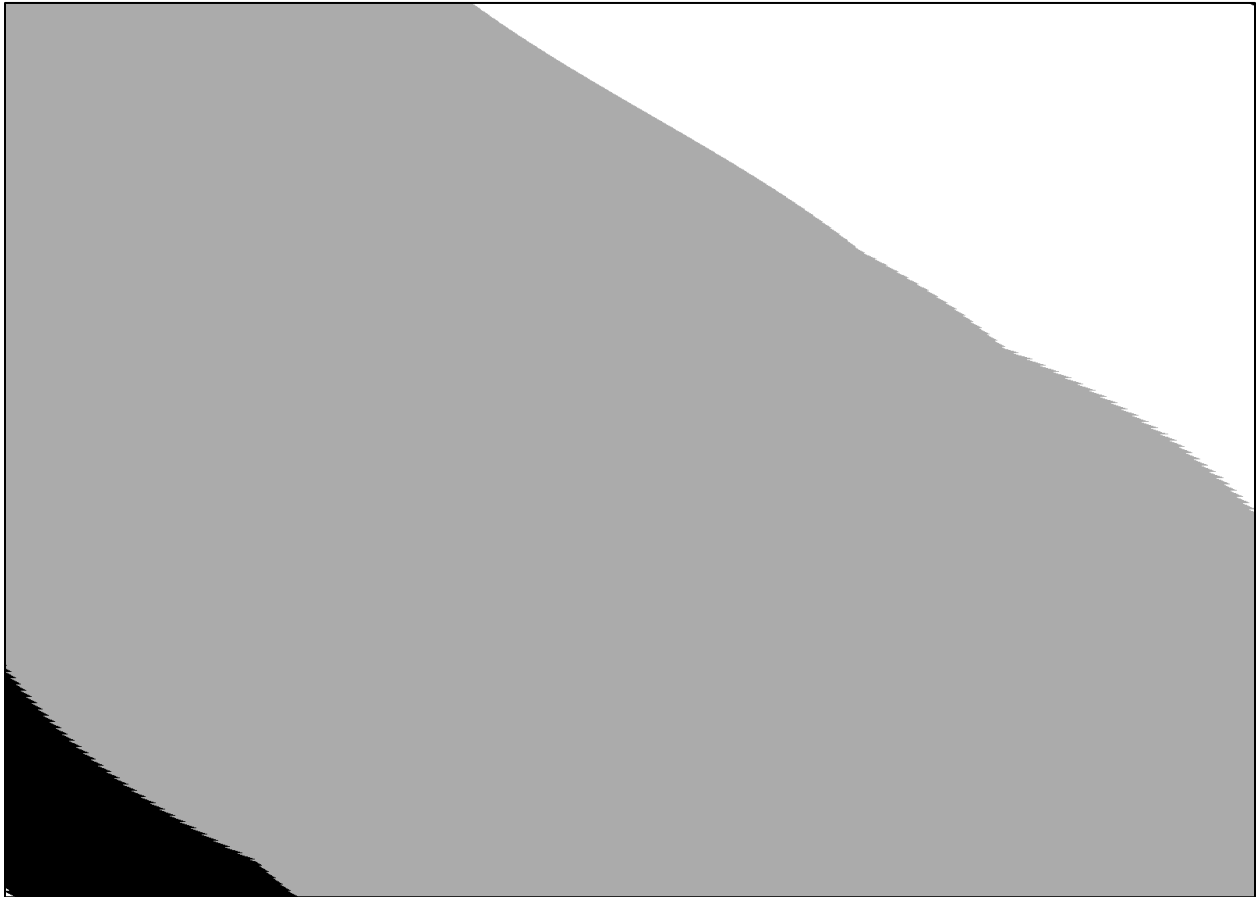


Figure 10. The solar zenith screen for the swath shown in Figures 4, 5 and 7. Night, solar zenith  $> 85^\circ$  in black, solar zenith  $85^\circ$  to  $70^\circ$  in gray and solar zenith  $< 70^\circ$  in white. A large extent of this swath has low illumination conditions, gray area, over the snow covered landscape.

The VPN10 algorithm outputs for NDSI snow cover, basic QA and QA bit flags are shown in Figs. 11, 12 and 13 respectively, for the VIIRS swath shown in Fig. 4.

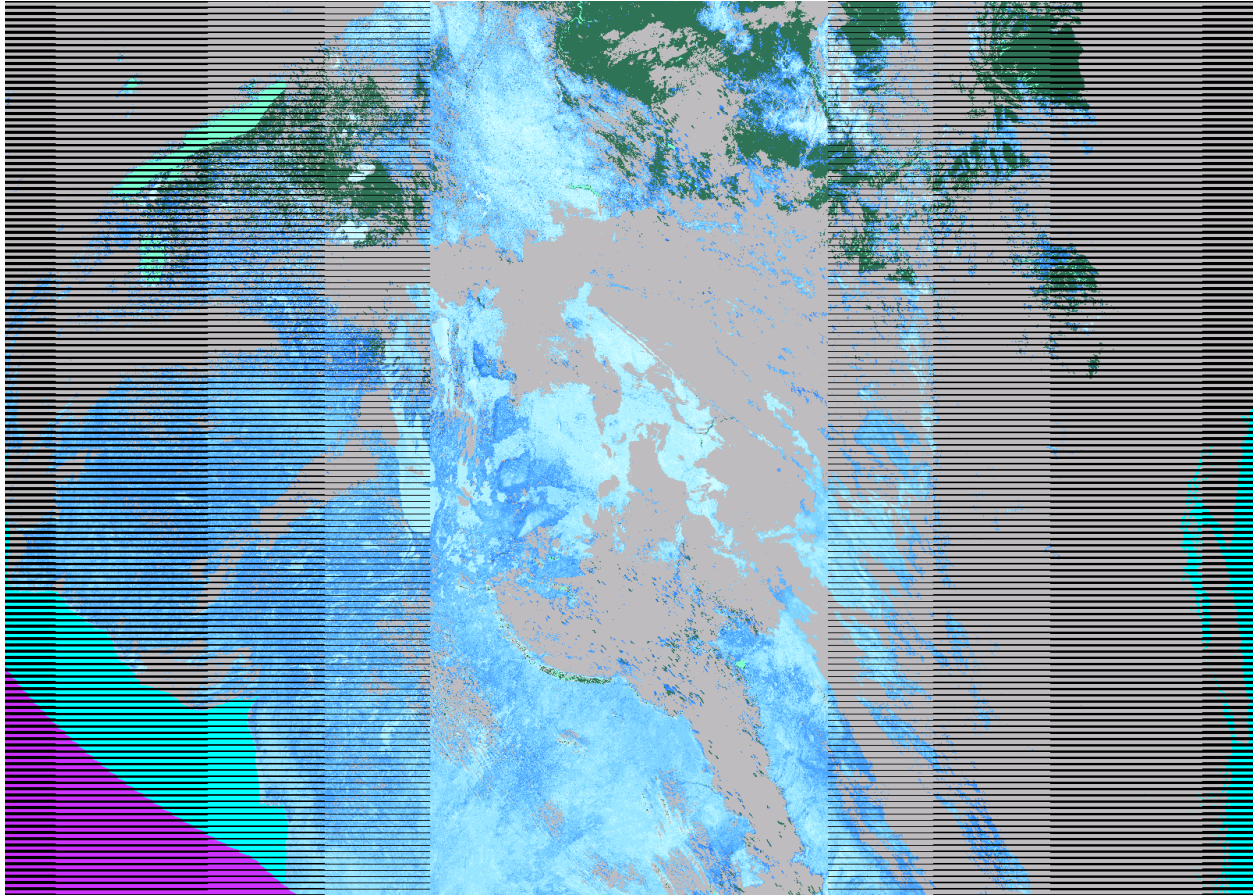


Figure 11. NDSI snow cover map for swath of 2014339.1945. NDSI snow cover in shades of blue from dark blue 1% to white 100%. Snow free land, green. Clouds masked in gray, oceans in cyan and night in purple.

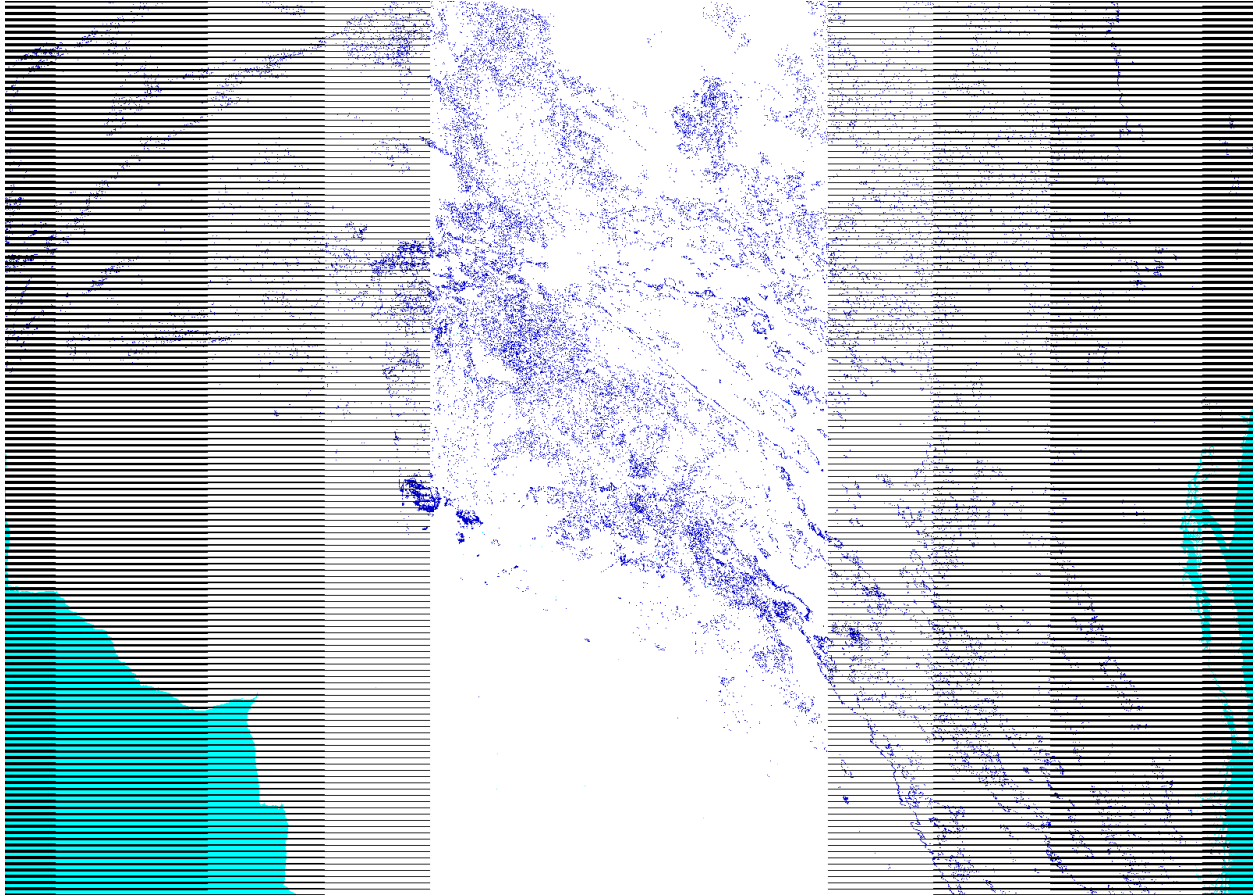


Figure 12. Basic QA for swath of 2014339.1945. Best quality in white, good in blue, poor in red. Oceans shown in cyan.

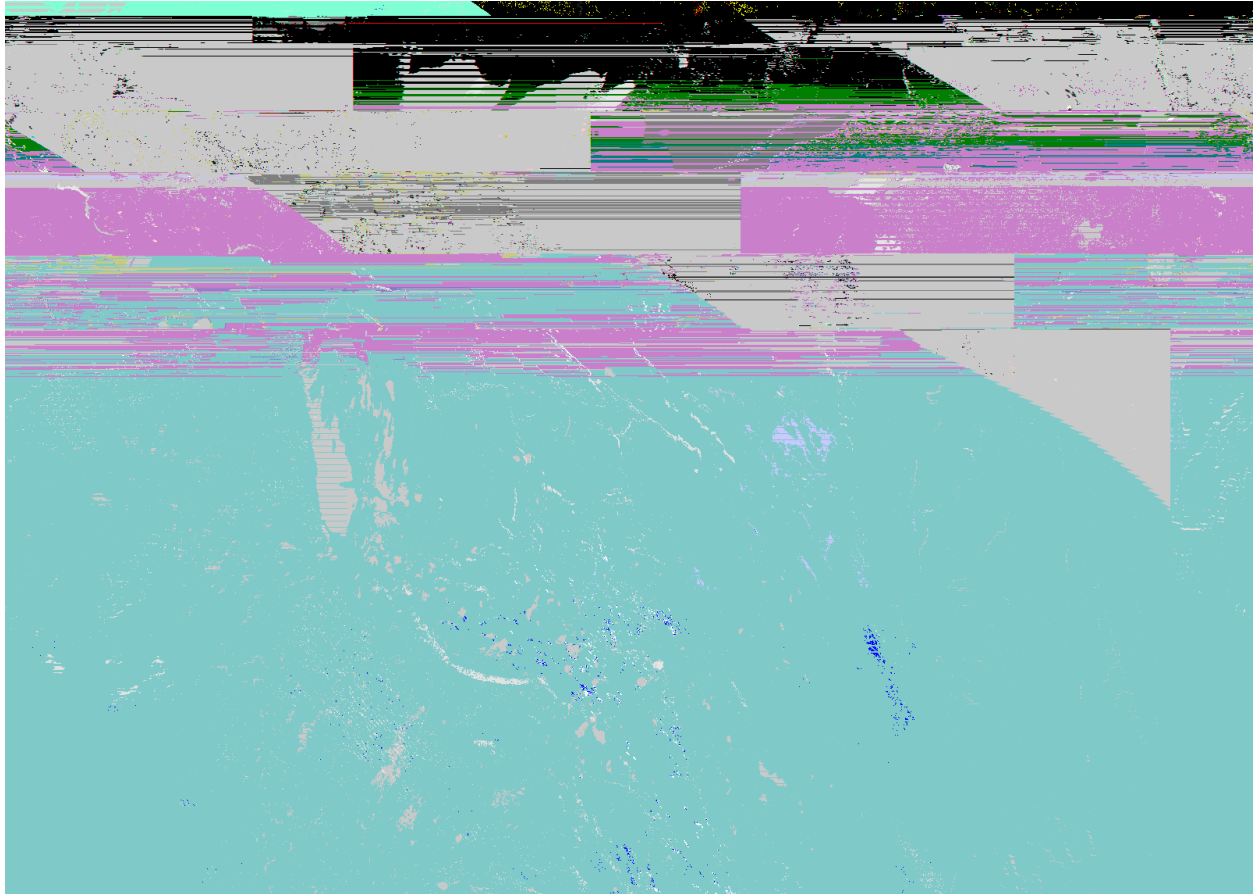


Figure 13. QA bit flags for swath of 2014339.1945. The region covered in cyan has the high solar zenith flag set to on and within that region gray is snow covered inland water, dark blue is snow detection with high SWIR screen set on. Snow detection is reversed by low VIS screen or low NDSI screen shown in red and yellow, respectively. Black represents where no bit flags are set. Note: there is no bit flag set for bowtie trim pixels.

## 4.0 PRODUCT ACCURACY/UNCERTAINTY

The accuracy of snow detection in clear sky conditions, favorable viewing geometry and illumination, has been estimated at 95% and greater throughout development and testing of the algorithm based on visual analysis with imagery and comparison to external snow cover maps. Accuracy applies to the mapping of snow covered area on the landscape. Uncertainty applies to detection of snow cover at the pixel level. Accuracy/uncertainty of the VIIRS snow cover product is very similar to that of the heritage MODIS snow cover product, C5 and C6. Literature reports regarding the MODIS snow cover products accuracy/uncertainty and the MODIS snow product user's guides (Riggs et al., 2006; Riggs and Hall, 2015) serve as the base to understanding VIIRS snow cover product accuracy/uncertainty. Accuracy of the heritage MODIS C5 daily snow cover product has been reported in the literature in several ways on a diversity of landscapes, with different methods of comparison, to ground data, or other snow cover map sources (e.g. Hall and Riggs, 2007; Marchane et al., 2015; Rittger et al., 2013;

Arsenault et al., 2012; Huang et al., 2011; Jain et al., 2008, more references can be found in the listing at the MODIS Snow and Sea Ice project <http://modis-snow-ice.gsfc.nasa.gov/?c=publications> or at the NSIDC listing of published research (<http://nsidc.org/data/modis/research.html>). The MODIS C5 snow cover accuracy has been reported over a range of 75% - 95% under clear-sky conditions and with caveats depending on the study.

Uncertainty of snow detection at the pixel level is affected by viewing conditions, land cover, amount of VIS and SWIR reflectance from the surface, and confidence in cloud detection. Causes of uncertainty in snow detection are screened for and flagged at the pixel level. See Sec. 3.2 for description of the screens applied. Uncertainty of snow detection can be assessed by reading the QA bit flags. If none of the bits are set then certainty of snow detection is high, if one or more of the bits are set then uncertainty is increased. The QA bit flags also can be read to determine why snow detection was reversed.

Snow commission errors, snow detection on non-snow features which are not blocked by any of the screens, have a negative impact on accuracy, primarily in a qualitative visual way when snow is seen in places where snow is impossible, e.g. the Southeast USA in August, however quantitatively snow commission occurs for very few pixels, typically <0.01% of a swath. Two causes of snow commission errors in the algorithm are the cloud mask and geologic surface features.

The VIIRS CMIP cloud confidence flag is used by the snow cover algorithm to mask clouds. If the cloud confidence flag is set to certain cloud for a pixel that pixel is masked as cloud. If the flag is set to certain clear or probably clear or probably cloudy the pixel is processed as clear view of the surface. The CMIP is gridded from its 750 m resolution to 375 m resolution of snow cover using nearest neighbor technique in the algorithm. This is a basic applied use of the CMIP; no assessment is made regarding the accuracy/uncertainty of the cloud confidence flag. If clouds in the scene are not identified as certain cloud then it is possible that snow detection errors can be made because there is cloud reflectance mixed in the reflectance for a pixel. Relative to snow detection, undetected subpixel clouds can result in snow commission errors because cloud reflectance mixed with other features can give an NDSI > 0.0 and has reflectance features similar to snow that pass through those screens, and the cloud can reduce the estimated surface temperature to below the threshold of the surface temperature screen. Thus snow commission errors are often associated with popcorn, scattered, broken cloud conditions or along edges of solid cloud formations creating cloud mixed pixels. An example of the situation is shown in Fig. 9 with snow commission errors remaining after all the screens have been applied.

Snow cover omission errors can occur when the CMIP flags snow cover as certain cloud despite clear skies. We have investigated that situation (Riggs and Hall, 2003), and continue to investigate that situation. Often that is a result of the CMIP or the heritage MODIS cloud mask ancillary snow/ice background input data set missing the snow cover which results in the cloud

algorithm following a snow free processing path and erroneously detecting snow as cloud. In brief, the CMIP algorithm begins with an initial guess of the land surface as snow free or snow covered based on its internal snow cover detection algorithm and if necessary ancillary snow cover maps that guess of surface state directs subsequent cloud detection processing and cloud tests applied. Investigation of the CMIP processing path and cloud test flags has found that in these situations the CMIP algorithm started from a snow free land state and detected certain cloud by a single visible spectral test. A possible solution to that problem has been developed and is being tested for accuracy and reliability. Cloud/snow confusion issues are discussed with the UW cloud mask algorithm developers as well as ways to accurately discriminate between clouds and snow. In this algorithm version this snow cover omission error associated with cloud/snow confusion is not specifically addressed in any way.

Geologic surface features such as salt flats, e.g. Bonneville Salt Flats, UT, can have reflectance characteristics similar to snow thus may cause snow commission error. These are static features of the landscape, so are a persistent location of possible snow commission error. However, depending on the location and elevation, and seasonal temperature changes from below freezing to well above freezing of the feature, the surface temperature and height screen may reverse snow detections to not snow when the surface is warm but be ineffective when the surface is cold and snow free.

## **4.1 Uncertainty Estimate**

Certainty of snow detection with the NDSI depends on the amount of VIS and SWIR reflectance from snow and on the relative difference between the VIS and SWIR reflectance as discussed in Sec. 2.2 and shown in Fig. 4. In general as the NDSI value increases the certainty of snow detection increases. A way to quantitatively estimate uncertainty is to apply a sigmoid function which may be used to express the accuracy or perceived confidence of a snow detection based on the NDSI value. The perceived confidence can increase and decrease from any chosen NDSI value and the function parameters adjusted to show a change in perceived confidence. An NDSI value of 0.3 as the threshold above which snow detection has high confidence the sigmoid function in Fig. 14 shows the perceived confidence in snow detection. The NDSI value of 0.3 is chosen based on experience, evaluation and validation of with the MODIS and VIIRS data as a reasonably good threshold value from which to gauge accuracy.

The sigmoid function is not calculated in the algorithm so a user would need to calculate it to estimate uncertainty. From a user's perspective, an NDSI value relevant to their use can be selected and a sigmoid function applied to generate an estimated confidence surrounding that threshold as shown in Fig. 14. Determination of which NDSI value to select for a threshold depends on a user's need; NDSI values from 0.1 to 0.4 have been used in the literature (see Sec. 2.2) to make SCA maps. A user can use the sigmoid function to estimate uncertainty associated with an NDSI value selected as a threshold.

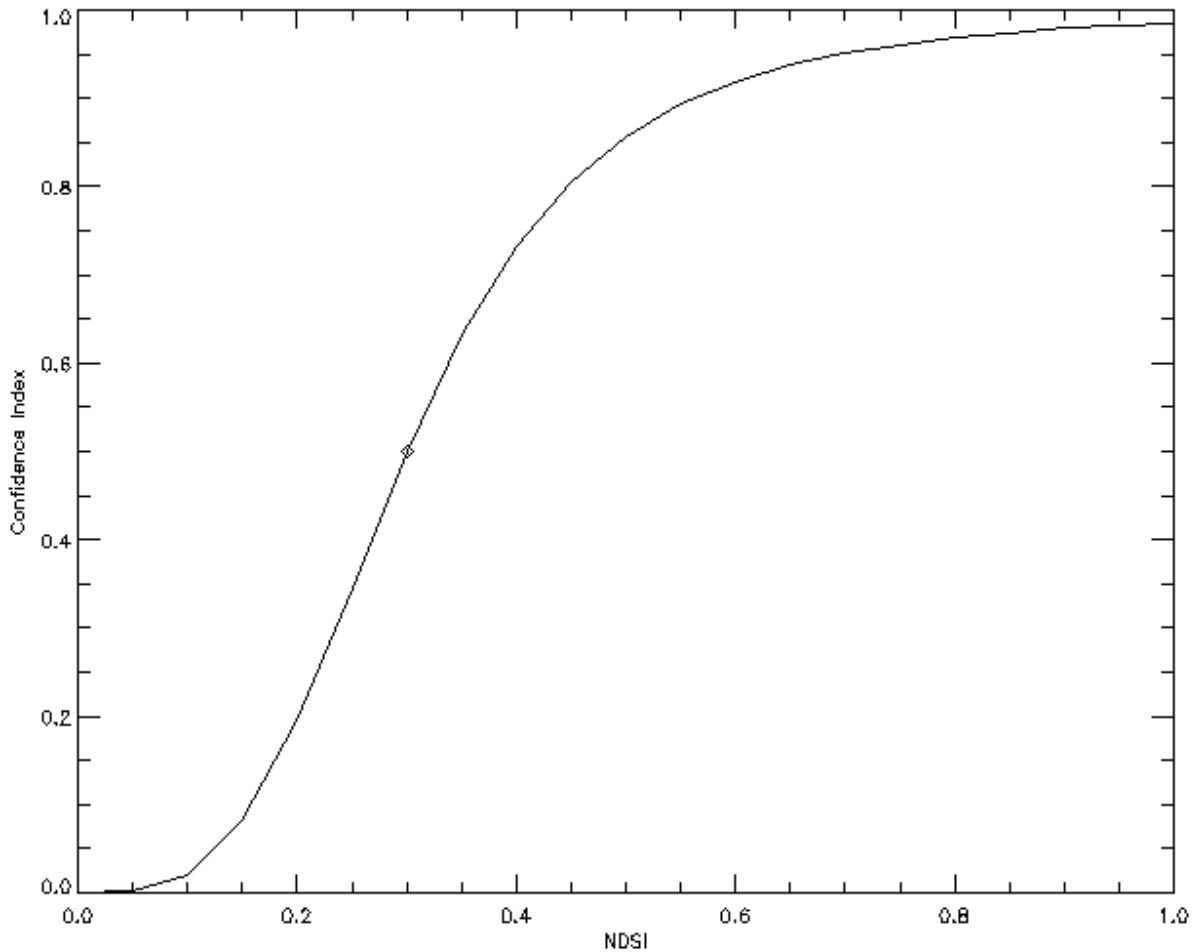


Figure 14. Estimated confidence surrounding the NDSI threshold set at 0.3 with half maximum confidence set at 0.5.

## 4.2 Validation Approach

To validate the product, the uncertainties in snow detection at the pixel level will be defined and the accuracy of extent of snow cover across the landscape mapped in the data product will be assessed against ground station data (ground truth) and snow cover extent maps from external sources, and visual interpretation of VIIRS imagery. Validation of snow cover extent via ground truth and other snow cover extent maps is important relative to the intended uses of the data product. Uncertainties in snow detection at the pixel level within the algorithm are well understood, described in previous sections and QA bit flags are set to alert users to algorithm results and uncertainty of snow detection.

Validation with ground truth, a surface point measurement of snow depth and/or snow water equivalent (SWE), compared to a 375 m spatial resolution VIIRS pixel should consider local conditions at the site because location of the station may or may not be a good representation of



the surface features and snow cover in the local area seen in the VIIRS pixel. Also, geolocation accuracy of VIIRS data can be a factor. Studies validating the MODIS 500 m snow cover product with station snow cover depth data have described and dealt with these issues e.g. Aresenault et al. (2012). Comparison of VIIRS snow cover product with selected station data sources in several landscapes and at different times of a snow season will be done to establish product accuracy.

Comparative assessment of the VIIRS snow cover product across a landscape, e.g. plains, boreal forest, mountains, to other snow cover extent maps derived from satellite observations, or from station data or combination of satellite observations and station data, will be done to establish product accuracy at regional and global scales. The NOAA National Ice Center (NIC) Interactive Multisensor Snow and Ice Mapping System (IMS) daily snow cover charts are a reliable data product that can be used for validation.

## 5.0 DATA FORMAT

### 5.1 Format

The snow cover data will be stored as data layers with local attributes describing the data. The product will include metadata relevant to archive, data identification, provenance/processing history and data quality of the product. The data product format will be HDF5.

Table 4. Listing of data layers in the snow cover data products.

Data Product	Data Layers
VNP10 (4 layers)	Snow Cover, Algorithm bit flags QA, Basic QA, NDSI
VNP10L2G (11 layers)	Snow cover, Algorithm bit flags QA, Basic QA, NDSI, orbit pointer, granule pointer, number of observations, Snow cover compact, Algorithm bit flags QA compact, Basic QA compact, NDSI compact,
VNP10A1 (6 layers)	Snow Cover, Algorithm bit flags QA, Basic QA, NDSI, orbit pointer, granule pointer
VNP10A2 (2 layers)	Maximum snow cover extent, day snow flag
VNP10C1 (3 layers)	Snow cover, Cloud cover, data quality flag

### 5.2 QA Metadata

QA metadata is written as global attributes that provide information on overall summary quality of the product, such as the percentage of good data processed in a swath.

## 6.0 PRODUCT PUBLICATIONS

A NASA VIIRS snow cover data products user guide will be written and posted at the NSIDC DAAC.

Riggs, G.A. and Hall, D.K. 2015. An introduction to the new NASA Suomi-NPP VIIRS snow cover data products, Proceedings of the 72nd Annual Eastern Snow Conference, Sherbrooke, Quebec, Canada.

Justice, C.O., Román, M.O., Csiszar, I., Vermote, E., Wolfe, R., Hook, S.J., Friedl, M., Wang, Z., Schaaf, C., Miura, T., Tschudi, M., Riggs, G., Hall, D.K., Lyapustin, A., Devadiga, S., Davidson, C., & Masuoka, E. (2013). Land and Cryosphere Products from Suomi NPP VIIRS: Overview and Status. *Journal of Geophysical Research-Atmospheres*, 118, 1-13, doi:10.1002/jgrd.50771.

## 7.0 REFERENCES

Arsenault, K.R., Houser, P.R. and De Lannoy, G.J.M. 2012. Evaluation of the MODIS snow cover fraction product. *Hydrological Processes*, doi:10.1002/hyp.9636.

Brown, R. D. and D. A. Robinson, 2011: Northern Hemisphere spring snow cover variability and change over 1922–2010 including an assessment of uncertainty, *The Cryosphere* 5: 219-229.

Brown, R.D., Derksen, C. and Wang, L. 2010. A multi-data set analysis of variability and change in Arctic spring snow cover extent, 1967-2008. *Journal of Geophysical Research* 115, D16111, doi:10.1029/2010JD013975.

Bunting, J. T., and d'Entremont, R. P., 1982. Improved cloud detection utilizing Defense Meteorological Satellite Program near infrared measurements, Air Force Geophysics Laboratory, Environmental Research Papers, No. 765, AFGL-TR-82-0027, 27 January 1982, 91 pp.

Burns P. and Nolin A. 2014. Using atmospherically-corrected Landsat imagery to measure glacier area change in the Cordillera Blanca, Peru from 1987 to 2010. *Remote Sensing of Environment* 140:165-178. Doi:10.1016/j.rse.2013.08.026.

Choi, G., Robinson, D.A. and Kang, S. 2010. Changing Northern Hemisphere Snow Seasons. *Journal of Climate*, 23:5305-5310, doi:10.1175/2010JCLI3644.1.

Crane, R. G., and Anderson, M. R., 1984. Satellite discrimination of snow/cloud surfaces. *International Journal of Remote Sensing*, 5(1), 213–223.

Crawford, C., 2013: Evidence for spring mountain snowpack retreat from a Landsat-derived snow cover climate data record, *The Cryosphere Discussions*, 7:2089-2117, [www.the-cryosphere-discuss.net/7/2089/2013/](http://www.the-cryosphere-discuss.net/7/2089/2013/).

Derksen, C. and Brown, R. 2012. Spring snow cover extent reductions in the 2008-2012 period exceeding climate model projections. *Geophysical Research Letters*, 39, L19504, doi:10.1029/2012GL053387.

Déry, S.J. and R.D. Brown RD, 2007: Recent Northern Hemisphere snow cover extent trends and implications for the snow-albedo-feedback. *GRL*, 34:L22504, doi: 10.1029/2007GL031474.

Dietz, A.J., Kuenzer, C. and Conrad, C. 2013. Snow-cover variability in central Asia between 2000 and 2011 derived from improved MODIS daily snow-cover products. *International Journal of Remote Sensing*, 34(11), 3879-3902. <http://dx.doi.org/10.1080/01431161.2013.767480>

Dietz, A.J., Wohner, C. and Kuenzer, C. 2012. European snow cover characteristics between 2000 and 2011 derived from improved MODIS daily snow cover products. *Remote Sensing* ISSN 2072-4292, doi:10.3390/rs4082432.

Dobreva, I. and Klein, A.G. 2011. Fractional snow cover mapping through artificial neural network analysis of MODIS surface reflectance. *Remote Sensing of Environment*, 115:3355-3366, doi:10.1016/j.rse\_2011.07.018.

Dozier, J., 1989. Spectral signature of alpine snow cover from the Landsat Thematic Mapper. *Remote Sensing of Environment*, 28, 9–22.

Frei, A., Tedesco, M., Lee, S., Foster, J., Hall, D.K., Kelly, R. and Robinson, D. 2012. A review of global satellite-derived snow products. *Advances in Space Research*, 50(2012) 1007-1029. doi:10.1016/j.asr.2011.12.021.

Hall, D. K., Riggs, G. A., and Salomonson, V. V., 1995. Development of methods for mapping global snow cover using Moderate Resolution Imaging Spectroradiometer (MODIS) data. *Remote Sensing Environment*, 54, 127–140.

Hall, D. K., Riggs, G. A., Salomonson, V. V., DiGirolamo, N. E., and Bayr, K. J., 2002. MODIS snow-cover products. *Remote Sensing of Environment*, 83, 181–194.

Hall, D. K., and Riggs, G. A., 2007. Accuracy assessment of the MODIS snow-cover products. *Hydrological Processes*, 21, 1534–1547.

Hall, D.K., Foster, J.L., DiGirolamo, N.E. and Riggs, G.A. 2012. Snow cover, snowmelt timing and stream power in the Wind River Range, Wyoming, *Geomorphology*, 137:87-93 doi:10.1016/j.geomorph.2010.11.011.

- Hall, D.K. and Riggs, G.A. 2011. Normalized-Difference Snow Index (NDSI) in Encyclopedia of Earth Sciences, Encyclopedia of Snow, Ice and Glaciers, Eds. V.P. Singh, P. Singh and U.K. Haritashya, Springer Science+Business Media B.V. 2011.
- Hassan, Q.K., Sekhon, N.S., Magai, R. and McEachern, P. 2012. Reconstruction of Snow Water Equivalent and Snow Depth Using Remote Sensing Data. *Journal of Environmental Infomatics*, 20(2); 67-74. Doi:10.3808/jei.201200221.
- Huang, X., Liang, T., Zhang, X. and Guo, Z. 2011. Validation of MODIS snow cover products using Landsat and ground measurements during the 2001-2005 snow seasons over northern Xinjiang, China. *International Journal of Remote Sensing*, 32(1):133-152. Doi:10.1080/01431160903439924.
- Jain, S.K., Goswami, A. and Saraf, A.K. 2008. Accuracy assessment of MODIS, NOAA and IRS data in snow cover mapping under Himalayan conditions. *International Journal of Remote Sensing*, 1-16, doi:10.1080/01431160801908129.
- Klein, A.G., Hall, D.K. and Riggs, G.A. 1998. Improving snow cover mapping in forests through the use of a canopy reflectance model, *Hydrological Processes*, 12:1723-1744.
- Kolberg, S. and Gottschalk, L. 2010. Interannual stability of grid cell snow depletion curves as estimated from MODIS images., *Water Resources Research*, 46:W11555, doi:10.1029/2008WR007617.
- Kyle, H. L., Curran, R. J., Barnes, W. L., and Escoe, D., 1978. A cloud physics radiometer, Third Conference on Atmospheric Radiation, American Meteorological Society, 28-30 June 1978, Davis, Calif., p. 107.
- Lin, J., Feng, X., Xiao, P., Li, H, Wang, J. and Li, Y. 2012 Comparison of snow indexes in estimating snow cover fraction in a mountainous area in northwestern China. *IEEE Geoscience and Remote Sensing Letters*, 9(4), 725-729. Doi: 10.1109/LGRS.2011.2179634.
- Machane, A., Jarlan, L., Hanich, L., Boudhar, A., Gascion, S., Taternier, A., Filali, N. LePage, M., Hagolle, O. and Berjamy, B. 2015, Assessment of daily MODIS snow cover products to monitor snow cover dynamics over the Moroccan Atlas mountain range, *Remote Sensing of Environment* 160;72-86 doi:10.1016/j.rse.2015.01.002.
- Metsämäki, S.J, Anttila, S.T., Markus, H.J. nad Vepsälä, J.M. 2005. A feasible method for fractional snow cover mapping in boreal zone based on a reflectance model. *Remote Sensing of Environment*, 95:77-95. Doi:10.1016/j.rse.2004.11.013. doi:10.1016/j.rse.2012.04.010.
- Metsämäki, S.J, Mattila, O.P., Pulliainen, J. Niemi, K. Luojus, K. and Böttcher. 2012. An optical reflectance model-based method for fractional snow cover mapping applicable to continental scale. *Remote Sensing of Environment*, 123:508-521.

- Mishra, V.D., Neghi, H.S., Rawat, A.K., Chaturvedi, A. and Singh, R.P. 2009. Retrieval of sub-pixel snow cover information in the Himalayan region using medium and coarse resolution remote sensing data. *International Journal of Remote Sensing*, 30:18, 4707-4731, doi: 10.1080/01431160802651959
- Negi, H.S., Singh, S.K., Kulkarni, A.V. and Semwal, B.S. 2010. Field-based spectral reflectance measurement of seasonal snow cover in the Indian Himalaya, *International Journal of Remote Sensing*, 31:9, 2393-2417, doi: 10.1080/01431160903002417.
- Nolin, A.W. 2010. Recent advances in remote sensing of seasonal snow. *Journal of Glaciology*, 56(200): 1141-1150.
- Painter, T.H., Rittger, K., McKenzie, C., Slaughter, P., Davis, R.E. and Dozier, J. 2009. Retrieval of subpixel snow covered area, grain size, and albedo from MODIS. *Remote Sensing of Environment*, 113:868-879. Doi:10.1016/j.rse.2009.01.001.
- Parajka, J. and Blöschl, G. 2012. MODIS-based snow cover products, validation, and hydrologic applications. In: *Multiscale Hydrologic Remote Sensing Perspectives and Applications*, Ed. N.Chang and Y. Hong, CRC Press, 978-1-43-987745-6.
- Pu, Z., L. Xu and V. Salomonson, 2007: MODIS/Terra observed seasonal variations of snow cover over the Tibetan Plateau, *GRL*, 34:L06706, doi:10.1029/2007GL029262.
- Punia, M. and Dhankar, V. 2014. Mapping of snow spectral properties and regional climatic variability in Alaknanda Baisin, Uttarakhand, India, No. 356/ISRS Proceedings 2014/ISPRSTCVIII Mid-Symposium, Hyderabad, India.
- Racoviteanu, A.E., Arnaud, Y., Williams, M.W. and Ordoñez. 2008. Decadal changes in glacier parameters in the Cordillera Blanca, Peru, derived from remote sensing, *Journal of Glaciology*, 54(186), 499-510. Doi:10.3189/002214308785836922.
- Rittger, K., Painter, T.H. and Dozier J. 2013. Assessment of methods for mapping snow cover from MODIS. *Advances in Water Resources*, 51:367-380. Doi:10.1016/j.advwatres.2012.03.002.
- Riggs, G. A., Hall, D. K., Barker, J. L., and Salomonson, V. V., 1993. The Developing Moderate Resolution Imaging Spectroradiometer (MODIS) Snow Cover Algorithm, *Proceedings of the 50th Annual Eastern Snow Conference*. 8–10 June. Quebec, Canada: Quebec City, pp. 51–58.
- Riggs, G.A., Hall, D.K, and Salomonson, V.V. 2006. MODIS Snow Products User Guide to Collection 5, <http://modis-snow-ice.gsfc.nasa.gov/?c=userguides>
- Riggs, G.A., and Hall, D.K. 2015. MODIS Snow Products User Guide to Collection 6. <http://modis-snow-ice.gsfc.nasa.gov/?c=userguides>

Riggs, G. and Hall, D.K. 2014. Tracking seasonal Appalachian snow cover with MODIS daily snow cover product. Proceedings of the 71<sup>st</sup> Annual Eastern Snow Conference, 3-5 June 2014, Boone, NC.

Riggs, G.A. and Hall, D.K., 2003. Reduction of cloud obscuration in the EOS MODIS Snow Data Product, Proceedings of the 60th Annual Eastern Snow Conference, Sherbrooke, Quebec, Canada, 4-6 June 2003.

Robinson D. and T. Estilow, 2013: 2013 Arctic report card: spring snow cover below average again, Climate.gov URL [www.climate.gov/news-features/featured-images/2013-arctic-report-card-spring-snow-cover-below-average-again](http://www.climate.gov/news-features/featured-images/2013-arctic-report-card-spring-snow-cover-below-average-again).

Rosenthal, W., and Dozier, J., 1996. Automated mapping of montane snow cover at subpixel resolution from the Landsat Thematic Mapper. *Water Resources Research*, 32(1), 115–130.

Salomonson, V.V. and I. Appel, 2004: Estimating the fractional snow cover using the normalized difference snow index, *Remote Sensing of Environment*, 89(3):351-360.

Salomonson, V.V. and I. Appel, 2006: Development of the Aqua MODIS NDSI fractional snow cover algorithm and validation results. *IEEE Transactions on Geoscience and Remote Sensing*, 44(7):1747-1756

Satterwhite, M.B., Mitchell, H., Hemmer, T. and Leckie, J.D. 2003. Field spectral signatures of snow, ice and water. Algorithms and Technologies for Multispectral, Hyperspectral and Ultraspectral Imagery, IX, S.S. Shen and P.E. Lewis eds., Proceedings of SPIE 5093.

Sibandze, P. Mhangara, P., Odindi, J. and Kganyago, M. 2014. A comparison of Normalized Difference Snow Index (NDSI) and Normalized Difference Principal Component Snow Index (NDPCSI) techniques in distinguishing snow from related land cover types. *South African Journal of Geomatics*, 3(2) 197-209, doi: <http://dx.doi.org/10.4314/sajg.v3i2.6>

Valovcin, F. R., 1976. Snow/cloud discrimination, AFGL-TR-76-0174, ADA 032385.

Valovcin, F. R., 1978. Spectral radiance of snow and clouds in the near infrared spectral region, AFGL-TR-78-0289, ADA 063761.

Yin, D., Cao, X., Chen, X., Shao, Y., and Chen, J. 2013. Comparison of automatic thresholding methods for snow-cover mapping using Landsat TM imagery, *International Journal of Remote Sensing*, 34:19, 6529-6538, doi: 10.1080/01431161.2013.803631.

Zhang, J. and Zhou. 2011. Spectra reflectance characteristics of different snow and snow-covered land surface objects and mixed spectrum fitting. IEEE Committees of “2011 International Conference on Geoinformatics” Doi:10.1109/GeoInfomatics.2011.5980696.